International Journal of Concrete Structures and Materials

RESEARCH Open Access

Experimental Testing and Numerical Simulation of Recycled Concrete Aggregate in a Concrete Mix

Bini Neupane[1], Kameshwar Sahani[1] and Shyam Sundar Khadka[1*]

Abstract

This study focuses on exploring the potential of utilizing demolished concrete and promoting sustainable practices through the use of recycled concrete aggregate (RCA) as a substitute for natural aggregates, particularly in the context of Nepal. The region's susceptibility to frequent earthquakes results in significant volumes of concrete rubble, posing challenges in waste disposal. To address this issue and mitigate resource depletion, the research focuses on concrete recycling. By conducting a thorough analysis of mechanical properties, crack patterns, strength variations, and specific gravity evaluations across different RCA compositions, the study emphasizes the ongoing endeavors toward sustainable concrete practices. A comparative examination of test results involving varying percentages of coarse recycled aggregate content (0%, 25%, 50%, 75%, and 100%) denoted as R0, R25, R50, R75 and R100, respectively, provides insights into the performance of different mixes. The compressive strength of cube for R25 increased by 20.13%, while R50 and R75 showed gains of 8.08% and 1.28%, respectively, while cylinder showed an increase of 25.86%, 18.88%, 9.54% and 2.65% for R25, R50, R75 and R100, respectively, compared to R0 concrete mix when tested at 28 days of curing. Tensile strength of concrete cylinder also improved, with R25 showing an 18.52% increase and R50 showing a 9.26% increase. Additionally, the RCA increased the flexural strength, with R25 leading with a 5% increase and R50 following with a 1.66% increase at 28 days of testing. The inclusion of numerical analysis in ABAQUS CAE using the Kent and Park Model serves to reinforce and support the experimental findings, establishing the credibility of both approaches. In essence, the study strongly advocates for the integration of recycled aggregate in concrete as a means to foster sustainable development and environmentally friendly construction methods.

Keywords Recycled concrete aggregate (RCA), Natural coarse aggregate (NCA), ABAQUS, Concrete damage plasticity (CDP), Recycled aggregate concrete (RAC)

1 Introduction

Concrete production in the world is increasing each year, which has a significant impact on water consumption, natural aggregates and cement production. De Brito et al., (2019) state that 45 billion tons of natural aggregates were produced in 2017, and it is estimated that this figure will increase to 66 million tons by 2025. It is estimated that the construction industry accounts for around 40% of global resource consumption, with a significant portion of this, about one-third, being aggregates utilized in the production of cement-based products (Kalinowska-Wichrowska et al., 2022). The amount of aggregates consumed is about forty billion tons per year and represents the enormous development projects that are being carried out all over the world, which means huge sections of mountains have to be dug or dismantled in order to supply these materials (Tam et al., 2018).

Journal information: ISSN 1976- 0485 / eISSN 2234-1315.

*Correspondence:
Shyam Sundar Khadka
sskhadka@ku.edu.np
[1] Department of Civil Engineering, Kathmandu University, Dhulikhel, Nepal

Concrete consumption also leads to rapid concrete demolition of buildings and infrastructure, which takes place as a result of the removal of structures. The demolition of existing buildings for new construction or regeneration, the decommissioning of major infrastructure projects like bridges and dams, the removal of old pavement surfaces during road reconstructions as well as rehabilitation efforts resulting from renovation activities are also included. Another main cause of accumulation of demolished waste is natural disasters such as Earthquake.

There were 498,852 entirely destroyed homes and 256,697 partially damaged homes as a result of the 7.8 Richter scale Gorkha Earthquake 2015 on April 25 and the significant aftershock of 7.3 magnitude on May 12. There were four million tons of waste produced only in Kathmandu, which is approximately 11 years' worth of waste generated normally (Post Disaster Needs Assessment, 2015). Even after the earthquake, numerous non-engineered structures have been demolished, posing hazards to the safety of the people and the nation's reconstruction. As the country, lies on active tectonic plate, modern buildings have been built by using RC frames with brick masonry infill for the last 40 years. Not only buildings, but bridges which exceeds its life span are being demolished.

A 7.8 Mw earthquake struck southern, central Turkey and the north and west of Syria on 6 February 2023. The Ministry for Environment, Urbanization and Climate Change carried out inspections on 1.25 million buildings before 23 February 2023 which showed that 164,000 buildings had either been damaged or severely damaged. There was also a moderate degree of damage to another 150,000 business infrastructures. However, there is still a lack of appropriate technologies in place with regard to concrete and debris recycling. Concrete debris from destroyed buildings cannot degrade like biological waste. Thus, most of the concrete and debris is being disposed in near construction site after building demolition or used as road infill (Gonzalez-Valencia et al., 2016).

Utilizing demolished concrete could be a way to promote "sustainable development" and environmentally friendly construction methods. In general, demolished concrete is crushed in two stages, materials and pollutants such as paper, wood and reinforcement are screened and Recycled Concrete Aggregate (RCA) is prepared and when the RCA is used to prepare concrete then it is referred as Recycled Aggregate Concrete (RAC). According to Buck (1977), the early years of RCA use were at the end of World War II marked by widespread building and road demolition as well as an urgent need to rebuilt Europe and get rid of waste material. Developing economies began to take steps towards reducing construction and demolition waste during the 1980s, while Germany initiated a federal quality association for recycled building materials from 1984 (Tam et al., 2018).

Global research has extensively investigated the use of RCA as a substitute for natural aggregates in concrete (Srivastava et al., 2015); (Tabsh & Abdelfatah, 2009); (Rahal, 2007); (Malešev et al., 2010); (Gyawali, 2022); (Corinaldesi, 2011); (Xiao et al., 2005); (Etxeberria et al., 2007)). Xiao et al., (2005) found a reduction in compressive strength with varying levels of Natural Coarse Aggregate (NCA) replaced by RCA. Etxeberria et al., (2007) observed that concrete incorporating 25% RCA achieved comparable compressive and tensile strength to conventional concrete. Tabsh and Abdelfatah (2009) in 2009 reported nearly equivalent compressive strength for robust RCA at target strengths of 30 MPa and 50 MPa, but a 25–30% drop in tensile strength at 30 MPa. Malešev et al., (2010) reported increased compressive, tensile, and flexural strength for R50 and R100 mixes. Corinaldesi (2011) found a 20% strength loss at a 30% replacement with a water-cement ratio of 0.5. In 2022, Gyawali (2022) reused debris from the 2015 Gorkha Earthquake in Nepal, noting a decrease in compressive strength for 20% Saturated Surface Dry (SSD) brick aggregate but an increase for 20% Oven Dried (OD) aggregate. There was also a decrease in compressive strength for 10% and 20% recycled powder and fine aggregate.

Past studies indicate variations in the strength of concrete specimens, with (Tabsh & Abdelfatah, 2009) emphasizing the crucial role of RCA quality in this fluctuation. Quality RCA, considering factors like gradation and particle integrity, enhances concrete strength by promoting superior interfacial bonding and minimizing contaminants such as residual mortar. Another significant influence on RAC quality is the physical properties of RCA, including specific gravity, porosity, and water absorption. The presence of residual mortar affects these properties, leading to a lower specific gravity in RCA compared to Natural Aggregate ((Tabsh & Abdelfatah, 2009); (Rahal, 2007); (Malešev et al., 2010); (Corinaldesi, 2011); (Xiao et al., 2005); (Etxeberria et al., 2007); (de Juan & Gutiérrez, 2009); (Oikonomou, 2005); (Volz et al., 2014); (Silva et al., 2014); (Sagoe-Crentsil et al., 2001); (Gagg, 2014)). Additionally, the introduction of RCA increases the complexity of the Interfacial Transition Zone (ITZ) in recycled concrete. The ITZ1 is between the original virgin aggregate and old mortar while ITZ2 is between the old mortar and the new mortar paste as shown in Fig. 1. The ITZ, especially ITZ2 between old and new mortar, becomes a crucial factor influencing RAC properties ((Yue et al., 2020); (H. Zhang et al., 2019); (Makul, 2021); (Memon et al., 2022); (Otsuki et al., 2003); (Li et al., 2012); (Y. Zhang et al., 2021)). While (Li et al., 2012) and (Makul, 2021) research suggests the

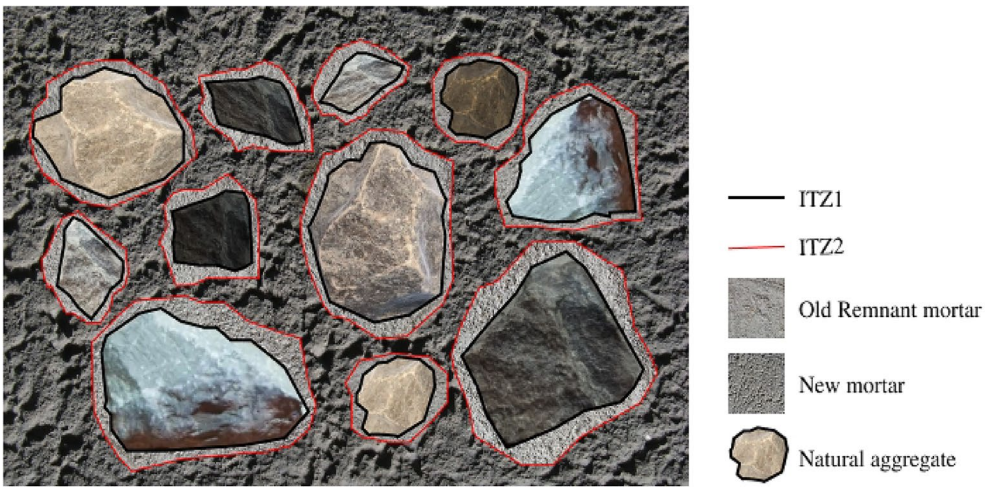

Fig. 1 Interfacial transition zone in recycled aggregate concrete

existence of more complex interface weak areas in recycled concrete, efforts have been proposed to enhance the mechanical properties of the ITZ and RACs for improved interfacial bonding and stress transfer.

The main goal of the study is to determine the mechanical properties of concrete containing Recycled Concrete aggregates (i.e., Compressive Strength, Tensile Strength and Flexural Strength). The other objective is to analyze the crack patterns of RAC and NAC concrete both experimentally as well as numerically and also to compare the strength variations for different concrete mix. To compare the physical properties of NCA and Demolished concrete and evaluate the specific gravity for different variations of RCA has also been a primary goal. It is generally not suggested to employ fine recycled aggregate (FRA) in structural concrete for the generation of RAC. The major drawbacks of FRA, such as decreased mechanical strength, problems with durability, and possible variations in the qualities of the concrete, are the primary causes of this concern. Therefore, FRA is often regarded as unsuitable for structural applications within RAC (Bravo et al., 2015; Evangelista & de Brito, 2010; Malešev et al., 2010; Zaharieva et al., 2003).

The goal of the current study is to design M20 concrete mix variations with five different RCA percentages. The M20 grade was selected because it offers a good mix between strength and workability and is widely used in Nepalese residential and commercial construction. The Nepal Building Code (NBC 105: 2020) states that M20 is the minimum grade needed for structural concrete, while M25 is necessary for structures taller than 12 m. This demonstrates how common and significant M20 concrete is in Nepal's building sector. In order to integrate recycled materials into the most widely used concrete grade in Nepal, this study investigates the usage of RCA in M20 concrete.

2 Experimental Program

2.1 Materials

Prior to casting the specimens in accordance with Indian Standard, the components of the design mix of concrete, including cement, fine aggregate, coarse aggregate, both natural and recycled concrete aggregates, were tested.

Locally available 43 grade Ordinary Portland Cement (OPC) with specific gravity 3.16 was the only cement used in the concrete production for the study that is readily available in the local market. Various Physical test for Hydraulic Cement has been performed as per IS:4031–1988: Methods of physical test for hydraulic Cement. These tests encompass various aspects of cement properties, guaranteeing that the chosen cement meets the specified standards for construction applications. Table 1 shows the various test of cement performed in laboratory:

A well graded river sand, which passed through a 4.75 mm sieve and met all the production criteria for concrete mixtures has been used in this study. The test required for the concrete mix production has been performed conforming to (IS383, 2016). The specific gravity and water absorption of sand has been obtained from Pycnometer test as per (IS, 2386-Part III, 1963). Sieve analysis, following the procedure outlined in (IS, 2386-Part I, 1963) was used to assess the distribution of particle sizes in fine aggregate which confirms to Zone II. The findings of test of fine aggregate are tabulated in Table 2, and Fig. 2 illustrates the particle size distribution of sand.

Both NCA and RCA had undergone tests to determine their various qualities as per (IS383, 2016). Old concrete

Table 1 Physical test of cement

Tests	Values	Quality requirement
Fineness of cement (IS 4031- Part1, 1996)	9.205%	< 10%
Normal consistency (IS 4031-Part4, 1988)	28.5%	26–33%
Initial setting time of cement (IS 4031-Part5, 1988)	65 min	–
Final setting time of cement (IS 4031-Part5, 1988)	410 min	–
Soundness of cement (IS 4031-Part3, 1988)	0.73 mm	< 10 mm

Table 2 Test results of fine aggregate

Tested property	Values	Remarks
Specific gravity	2.46	–
Water absorption	1%	–
Fineness modulus	2.95	–
Coefficient of uniformity (C_u)	6.5	> 6
Coefficient of curvature (C_c)	1	Between 1 and 3

was crushed to create the RCA. It was unknown how durable old concrete was. Detailed extraction process of RCA is dictated in Fig. 3. Hammers were used for the first crushing, and secondary crushing were done simultaneously as seen in Fig. 4. Only the aggregates retained by the IS 4.75 mm sieve and those that passed through the IS 20 mm sieve were used to determine the design mix proportion. Table 3 displays the findings of the experiment on physical and mechanical properties of NCA and RCA with respect to Indian Standards (IS, 2386-Part III, 1963) and (IS, 2386-Part IV, 1963).

Table 3 compares the properties of NCA and RCA. NCA has a higher specific gravity (2.73) compared to RCA (2.66), indicating that NCA is denser and potentially stronger. NCA also has lower water absorption (0.5%) compared to RCA (1.35%), suggesting that NCA is less porous and more durable. The Los Angeles Abrasion (LAA) value of 36.5% for NCA suggests better resistance to wear and tear compared to 41.3% for RCA, making NCA more suitable for high-wear applications. Similarly, the Aggregate Impact Value (AIV) is slightly better for NCA (20% vs. 21.4%), indicating marginally higher resistance to impact loads. These properties imply that while RCA can be utilized effectively, especially in lower load applications, adjustments in mix design and application

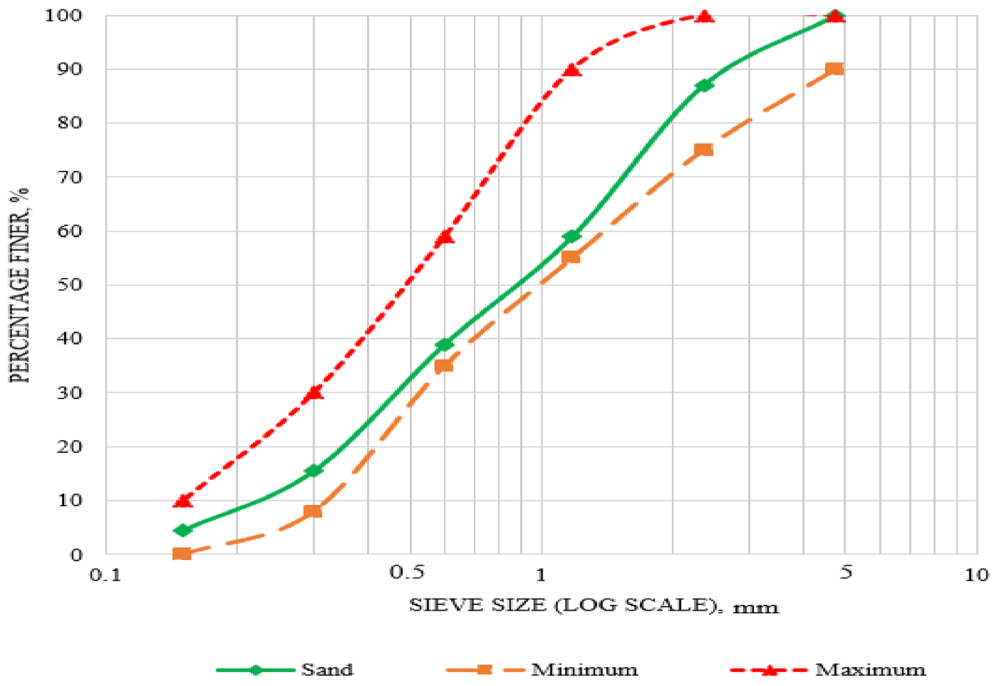

Fig. 2 Particle size distribution of sand

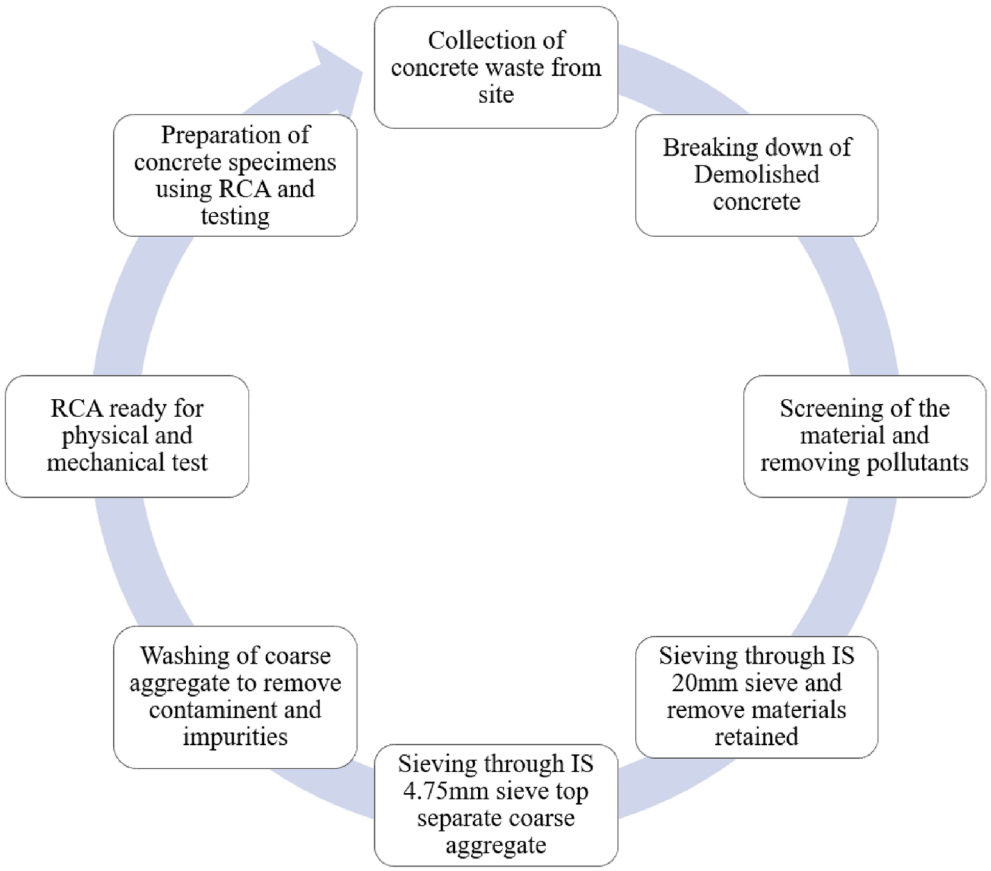

Fig. 3 Extracting process of recycled coarse aggregate

Fig. 4 Conversion of demolished concrete to recycled concrete aggregate; **a** crushing by hammer, and **b** final product RCA

Table 3 Results of coarse aggregate testing

Tested property	NCA	RCA
Specific gravity	2.73	2.66
Water absorption	0.5%	1.35%
Los Angeles abrasion value	36.5%	41.3%
Aggregate impact value (AIV)	20%	21.4%

Table 4 Results of sieve analysis

	NCA	RCA
Coefficient of uniformity (Cu)	2	2.29
Coefficient of curvature (Cc)	1.39	1.29

are essential to match the performance of NCA, particularly in high-traffic road construction where durability and resistance to wear and impact are critical.

Fig. 5 shows the gradation of Coarse Aggregate both Natural and Recycled. From Table 4, the coefficient of curvature for both Natural and recycled aggregate is between 1 and 3, therefore, both the aggregates are well graded.

2.2 Concrete Mixtures

The design mix for the study includes five different percentages of RCA in concrete with a grade of M20 and a water–cement ratio of 0.5. These percentages are R0 (0% RCA), R25 (25% RCA), R50 (50% RCA), R75 (75% RCA), and R100 (100% RCA). These percentages represent the replacement of NCA with RCA by weight. The quantities for the design mix, determined in accordance with (IS, 10262, 2019) are shown in Table 5. M20 grade concrete is a common classification used in India and other countries like Nepal, following Indian standards. It is characterized by a target compressive strength of 20 MPa after 28 days of curing. In practical applications, M20 grade concrete is widely used in Nepal due to its versatility and medium-strength properties. It finds frequent use in various construction projects such as residential buildings, small to medium-sized commercial structures, pavements, and similar applications. The mix ratio for M20 grade concrete typically involves combining 1 part cement, 1.5 parts sand, and 3 parts coarse aggregate.

According to Table 5, the given M20 concrete mix uses a higher cement content of 372 kg/m^3 (usually around 300–320 kg/m^3) due to the absence of chemical admixture. Without admixtures, more water is needed to maintain workability, raising the water–cement ratio from 0.533 to 0.558 as RCA content increases. The higher cement content compensates for this increased water, ensuring the concrete achieves the required strength and workability.

For the needed workability of RAC, NCA and RCA were first washed and oven dried for 4 h at a temperature

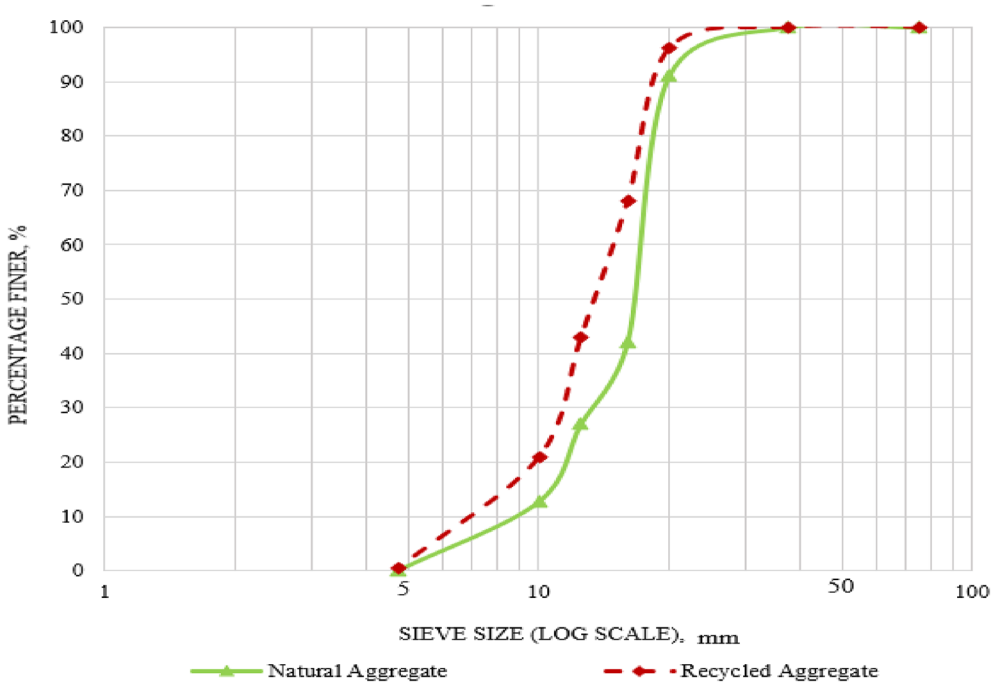

Fig. 5 Gradation curve of NCA and RCA

Table 5 Design mix quantities of component materials

Concrete mixture	R0	R25	R50	R75	R100
Cement (Kg/m^3)	372	372	372	372	372
Effective water (Kg/m^3)	186	186	186	186	186
Water–cement ratio taken (Kg/m^3)	0.5	0.5	0.5	0.5	0.5
Fine aggregate (Kg/m^3)	635.18	635.18	635.18	635.18	635.18
Natural coarse aggregate (Kg/m^3)	1155.82	866.86	577.91	288.95	0
Recycled coarse aggregate (Kg/m^3)	0	279.39	558.79	838.18	1117.57
Effective water–cement ratio	0.533	0.533	0.533	0.533	0.533
Total water–cement ratio	0.533	0.539	0.545	0.551	0.558
Additional water (Kg/m^3)	0	2.33	4.65	6.98	9.31
Chemical admixtures (Kg/m^3)	–	–	–	–	–
Slump (mm)	30	35	40	40	40
Final proportion of mix design	1:1.71:3.11	1:1.71:3.08	1:1.71:3.05	1:1.71:3.03	1:1.71:3.0

of 110 °C. Basic water content and additional water amount were then employed. In 24 h interval, the water absorption of recycled aggregates was tested. Based on the recycled aggregate's 24-h water absorption rate, additional water volume was determined. During the casting of the test specimen, slump value was found to increase from R0 to R50 and then constant at R50, R75 and R100.

Each mixture maintains a water–cement ratio of 0.5, with slight adjustments to accommodate the higher absorption of recycled concrete aggregates (RCA). This ensures suitable workability without the need for chemical admixtures, resulting in slump values ranging from 30 to 40 mm. While these slump values indicate relatively lower workability, they are manageable for specific applications. In situations with low workability, it is crucial to ensure thorough mixing and proper compaction to achieve the desired strength and durability. Regular checks for consistency and uniform distribution of materials are essential for maintaining concrete quality. Additionally, adequate curing practices can compensate for the lower workability and contribute to the overall performance of the structural concrete. Since the study is conducted without chemical admixtures, the current slump values are a reflection of this constraint. The addition of chemical admixtures would improve the workability of the concrete mixtures, enabling them to meet the broader requirements of real engineering applications.

Sample preparation, casting of specimen and slump test of all five concrete mix can be seen in Figs. 6 and 7, respectively.

2.3 Test Description

One of the goals of the experimental phase is to compare and investigate the physical characteristics of RCA and NCA, as well as the mechanical characteristics of concrete with various RCA percentages, such as compressive, tensile, and flexural strength.

A total of 120 concrete specimen were casted in laboratory which consists of:

- 45 cubes, each measuring 100 mm × 100 mm × 100 mm, for compressive strength testing at 7,14 and 28 days of curing.
- 15 cylinders of size 150 mm diameter and 300 mm height for testing compressive strength at 28 days of curing.
- 30 cylinders, sized 150 mm diameter and 300 mm in height, allocated for the split tensile test at 7 and 28 days of curing.
- For the Flexure strength test at 7 and 28 days post-cure, and additional 30 beams measuring 100 mm × 100 mm × 500 mm were prepared.

The weight of each specimen has also been taken into account to determine the bulk density for each concrete mixture.

3 Experimental Results and Discussion

3.1 Test Results

3.1.1 Compressive Strength Test

Five different variations of concrete mix of cubes and cylinders were tested in laboratory as seen in Fig. 8 as per (IS516, 1959), and the compressive strength was noted and their crack patterns were studied. Compressive strength for R25 concrete mix has been found to be highest. The strength increased from R0 to R25 but then decreased from R25 to R100. Despite this drop, all the concrete mixes with RCA showed higher compressive strength at 7, 14 and 28 days compared to the

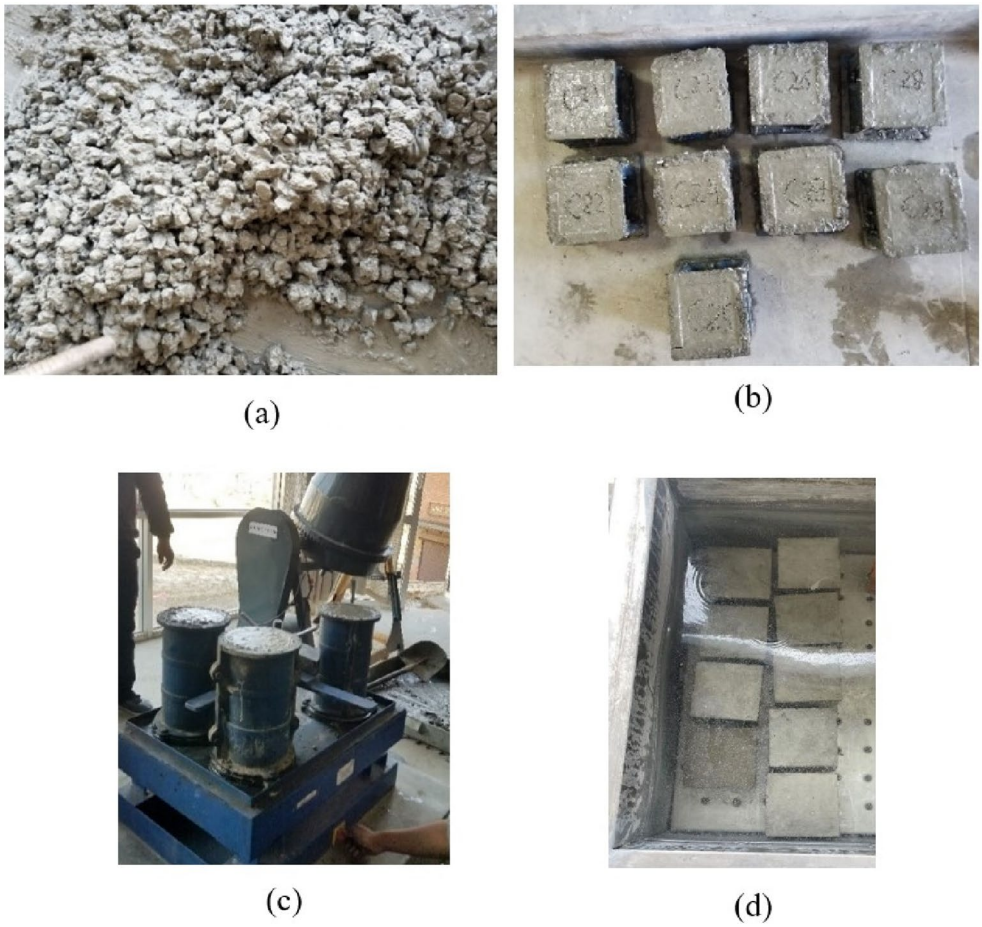

Fig. 6 Sample preparation and curing: **a** concrete mixing, **b** concrete cube casting, **c** compaction, and **d** curing

conventional mix. Table 6 presents the compressive strength of cylindrical and cubic specimens.

Fig. 9 illustrates that the failure process typically begins with the appearance of surface cracks. Initially, surface cracks form as a result of stress concentrations and microstructural weaknesses, exacerbated by lateral tensile stresses induced by the applied compressive load. As the load increases, these surface cracks propagate inward, extending along planes where the tensile stresses surpass the concrete's tensile strength. The most distinctive failure mode involves the formation of shear cracks at approximately 45-degree angles to the applied load, creating a characteristic cone-shaped failure pattern due to shear forces that exceed the material's shear strength.

As seen in Table 6, the compressive strength of cylinders was found to be less than that of cubes, as per the code. This discrepancy is due to geometric and stress distribution differences between the two shapes. Cubes have an aspect ratio (height-to-diameter ratio) of 1:1, while standard cylinders as seen in Fig. 10, typically have a 2:1 ratio. The lower aspect ratio of the cube results in a more evenly distributed stress across the entire cross-sectional area, leading to a higher average strength. Observing the ratios of f_{ck}/f_{cu} in Table 6, it can be seen that for the conventional concrete mix (R0), the ratio is 0.86, which nearly fits within the typical range of 0.8 to 0.85. However, for the other mixes incorporating Recycled Concrete Aggregate (RCA) (R25 to R100), the ratios are higher, ranging from 0.90 to 0.95. This can be explained by factors highlighted in the study (Yehia et al., 2020), which found that the cylinder to cube compressive strength ratio ranged from 0.78 to 0.93 depending on aggregate type and other variables. The RCA used in our research exhibits higher strength and lower water absorption itself compared to RCA used in other studies (Malešev et al., 2010; Tabsh & Abdelfatah, 2009; Xiao et al., 2005), leading to better bonding and compaction, and thus higher strength ratios.

3.1.2 Split Tensile Strength Test

Slit Tensile test of concrete is performed as per (IS5816, 1999), as seen in Fig. 11 where the force is applied on

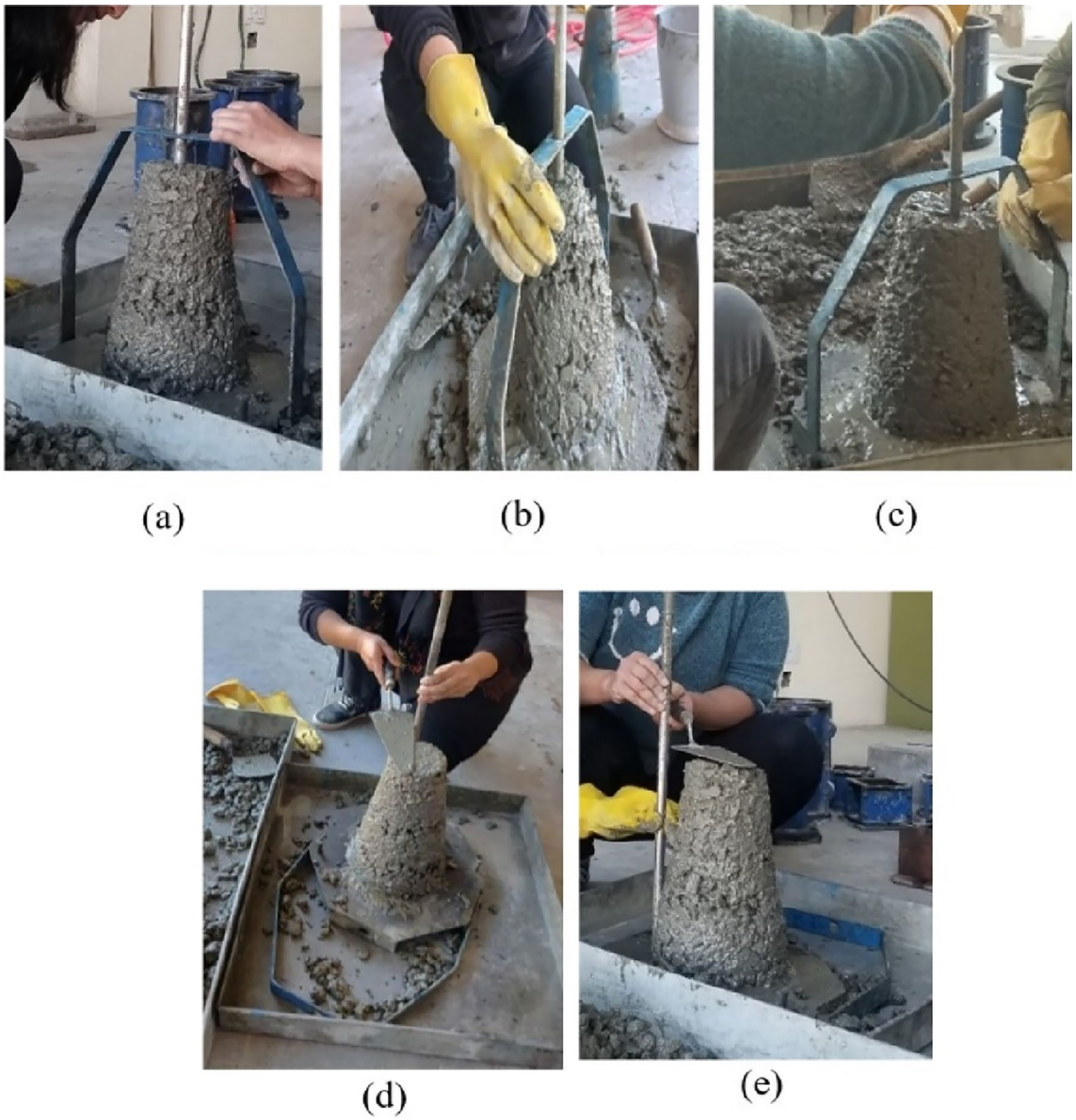

Fig. 7 Slump test: **a** R0, **b** R25, **c** R50, **d** R75 and **e** R100

the cylinder radially on the surface. The highest tensile strength was reported for R25 with a 25% RCA, and even R50 had a higher tensile strength than R0. The tensile strength of R75 and R100 is found to be almost no lower than that of R0. Splitting or Shear failure has been observed for all five concrete mixes which can be seen in Fig. 12. The applied compressive load induced tensile stresses in the central portion of the cylinder, perpendicular to the applied load. Cracking started to initiate and propagate in the cylinder as this tensile stress exceeded the tensile strength of concrete. The cracks eventually coalesced and merged, resulting in the separation of the cylinder into two halves along the vertical plane running the length of them. Table 7 shows the tensile strength for cylindrical specimens tested at 7 and 28 days of curing.

3.1.3 Flexure Strength Test

The PCC beam is also subjected to the (IS516, 1959) flexure strength test, which is intended to assess the flexural strength of a substance. After 7 and 28 days of curing, 30 samples of 5 different RCA variations were evaluated. This study used a four-point bend test as shown in Fig. 13, which involves applying force via two points on the top to make contact with the sample

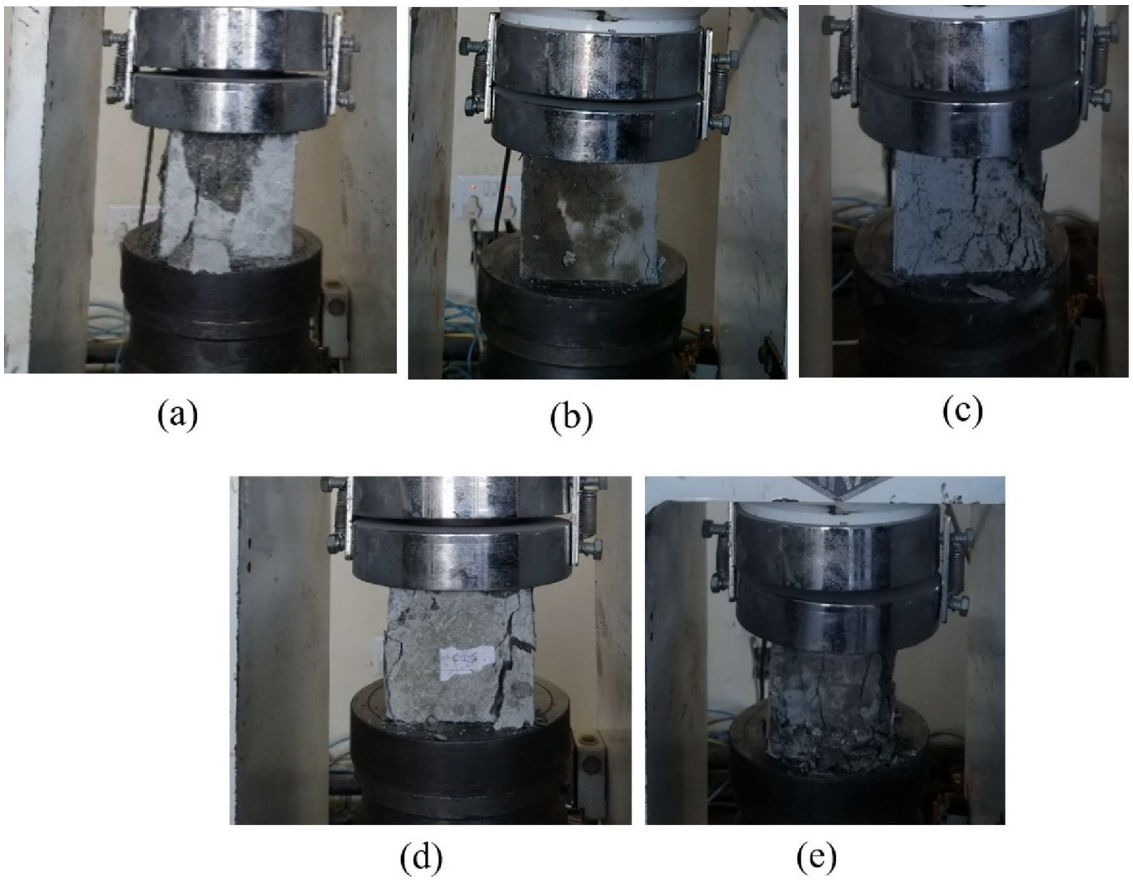

Fig. 8 Compressive strength test of cube performed in laboratory; **a** R0, **b** R25, **c** R50, **d** R75 and **e** R100

at four separate spots. Flexural Strength also presents a comparable set of results. The Modulus of Rigidity (MOR) for R25 is higher than that for the other concrete mix components. MOR is marginally higher than R0 for even R50 and R75. MOR for R100, however, was discovered to be somewhat lower than for R0. The cracks in the R0 mix were found to form in the middle of the beam, but in other variations, the crack's distance from the closer support was found to be decreasing in R25 and R50 beams and growing once again in R75 beams as per Fig. 14. The statistics from the beam specimen's four-point bend test are shown in Table 8:

Table 9 below compares the flexural strength of concrete, as determined by various empirical formulas, with the flexural strength obtained from our laboratory test for the R0 mix. The emperical formulas are sourced from different codes, providing a range of estimated values. The compressive strength of the concrete has been taken from Table 6 for the calculation of flexural strength.

Table 9 illustrates the flexural strength of concrete as determined by various empirical formulas compared to an experimental result of 3.61 MPa for R0. According to IS 456:2000, the flexural strength is calculated as 3.77 MPa, closely matching the experimental value. ACI 318 estimates a flexural strength of 3.11 MPa, while Eurocode 2 provides an estimate of 2.56 MPa. These results show the variability in predictions based on different codes and research, highlighting the range of methodologies used to estimate concrete flexural strength.

Table 6 Compressive strength of cube and cylinders

Concrete mix	Average compressive strength (MPa)				Ratio (f_{ck}/f_{cu})
	Cube			Cylinder	
	7 days	14 days	28 days (f_{cu})	28 days (f_{ck})	
R0	19.45	27.55	28.96	24.94	0.86
R25	25.78	31.62	34.79	31.39	0.902
R50	22.59	29.05	31.30	29.65	0.947
R75	21.54	27.68	29.33	27.32	0.931
R100	19.57	24.68	27.26	25.60	0.939

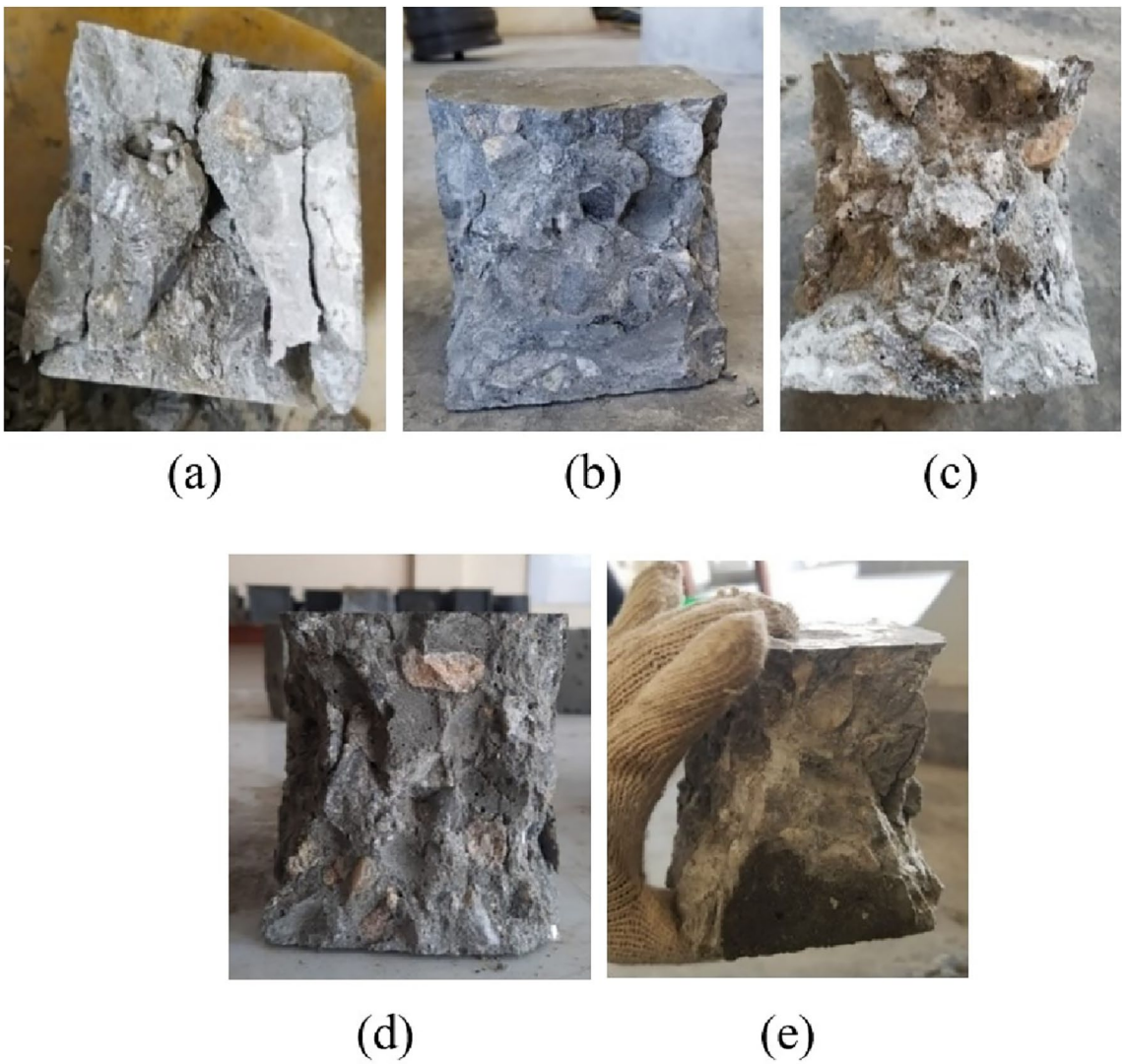

Fig. 9 Fracture patterns for compressive strength test of cube for different concrete mix: **a** R0, **b** R25, **c** R50, **d** R75 and **e** R100

3.1.4 Unit Weight

The unit weight of each concrete mixture was computed by taking the weight of each cylinder and beam specimen and dividing it by the volume of each specimen which is given in Table 10. Because the RCA in each concrete variation had a lower specific gravity than the R0, it was discovered that the unit weight decreased from R0 to R100.

3.2 Result and Validation

The analysis of the compressive strength tests, shown in Fig. 15, reveals a significant 4–5% increase in compressive strength for both R50 and R100 mixtures at 7 and 28 days, as reported by Malešev et al., (2010). In our current study, the compressive strength of the R50 mix showed a notable increase of 16.14% at 7 days and 8.08% at 28 days. However, for R100, we observed an insignificant strength increase at 7 days and a decrease of 5.87% at 28 days. These findings are in contrast to the results reported by Xiao et al., (2005), who noted a decrease in strength of 17.5% and 25.65% for R50 and R100 at 7 and 28 days, respectively.

The results of the 28 day Split Tensile test conducted by Malešev et al., (2010), illustrated in Fig. 16, demonstrated a significant improvement in tensile strength for the R50 mix, recording a 20.3% increase, and for the R100 mix, a 4.5% increase was observed. In our present study, we observed a noteworthy 9.26% enhancement in the tensile strength of the R50 mix over the 28 day testing period. However, in the case of the R100 mix, a marginal decrease of 1.39% in tensile strength was noted, which contrasts with the findings of Malešev et al., (2010).

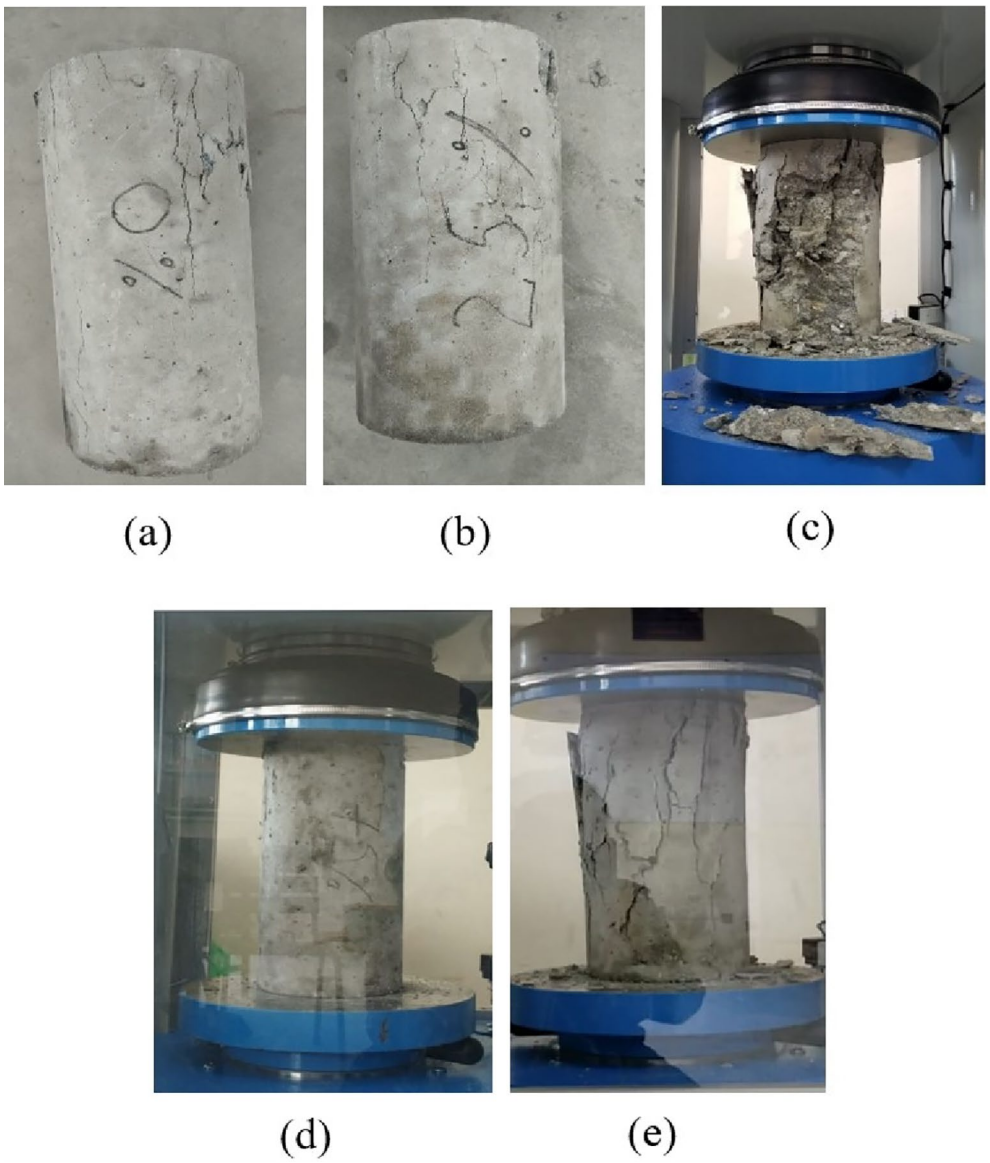

Fig. 10 Fracture patterns for compressive strength tests of cylinders for different concrete mix: **a** R0, **b** R25, **c** R50, **d** R75 and **e** R100

In the 28 day Flexure Strength test conducted by Malešev et al., (2010), a notable 5.56% increase in strength was observed, while for R100, there was a 3.7% decrease. Our current study reflects a comparable trend, with a slight increase of 1.66% in flexural strength for the R50 concrete mix and a decrease of 2.77% for the R100 mix, as depicted in Fig. 17. This aligns with the findings reported by Malešev et al., (2010).

Malešev et al., (2010) designed their concrete mix to achieve a compressive strength greater than 40 MPa at 28 days, while Xiao et al. targeted 32.5 MPa at 28 days. These target strengths differ significantly from the M20 concrete (20 MPa) examined in our study. Consequently, comparing percentage variations rather than actual strength values in MPa provides a more meaningful analysis. This approach normalizes the differences in target strengths, facilitating a clearer understanding of the relative performance improvements or declines in recycled aggregate concrete (RAC) compared to conventional concrete. Therefore, Figs. 15, 16, and 17 focus on percentage variations to highlight the relative performance rather than comparing with the actual values obtained.

In our research, we discovered that the RCA we tested showed satisfactory mechanical properties when compared to previous studies conducted by Malešev et al., (2010) and Xiao et al., (2005). This significantly

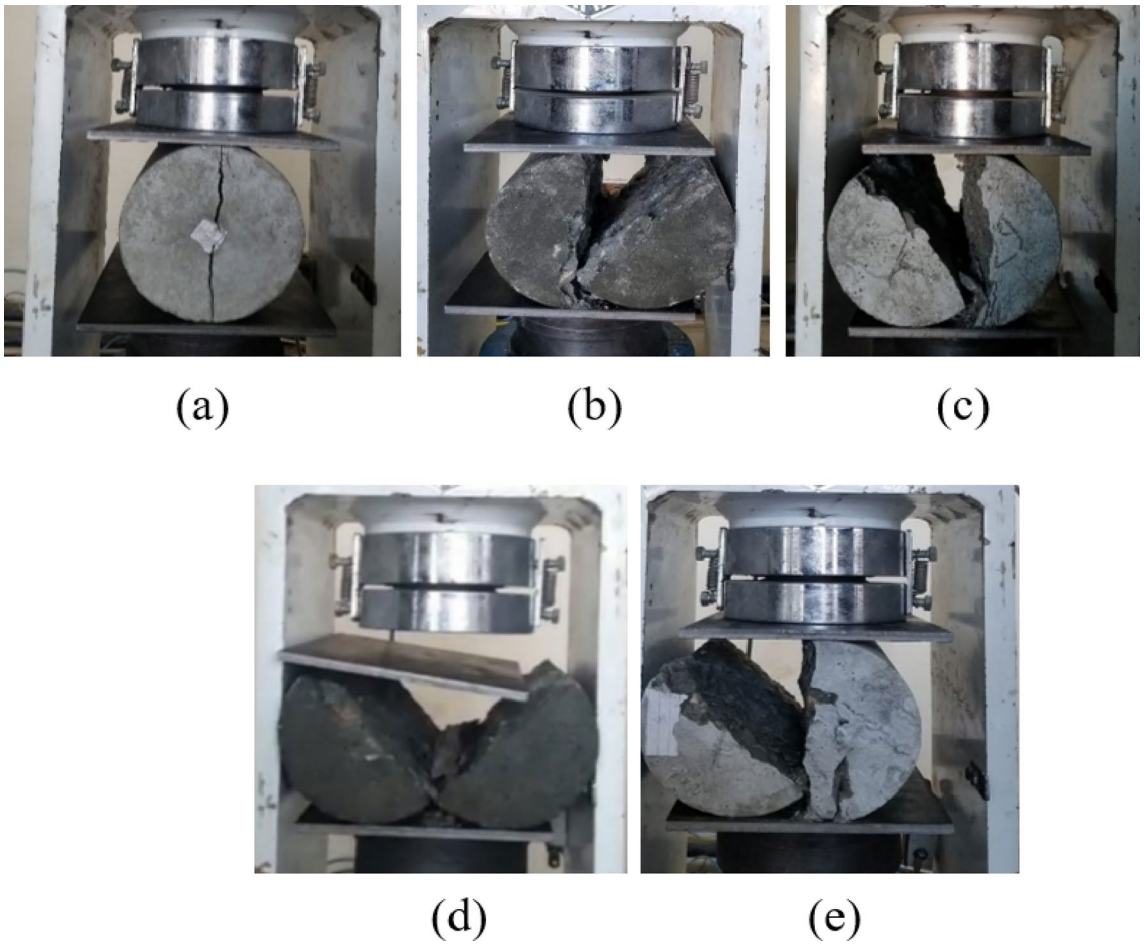

Fig. 11 Split tensile strength test of cylinders in laboratory; **a** R0, **b** R25, **c** R50, **d** R75 and **e** R100

contributed to the improved mechanical performance of our recycled aggregate concrete (RAC) mixes. The performance we observed can be largely attributed to the exceptional qualities of our RCA from Table 3. Specifically, our RCA had a specific gravity of 2.66, a water absorption rate of only 1.35%, a Los Angeles Abrasion (LAA) value of 41.3%, and an Aggregate Impact Value (AIV) of 21.4%. These characteristics indicate that the RCA we used was of high quality, which facilitated better bonding, compaction, and overall performance in our concrete mixes.

We noticed a distinct increase in the strength of our RCA concrete, which can be attributed to various factors, with the quality of the RCA being the most important. The rougher surface texture of the RCA, due to the presence of residual old mortar, played a vital role in improving mechanical interlocking and stress transfer with the new cement paste. This finding is aligns with previous research by Malešev et al., (2010), which supports the idea that the surface characteristics of RCA have a big impact on its performance in concrete mixes.

It is important to highlight that the variations in our study's data compared to previous literature may stem from differences in the mixing process and, crucially, the quality of the RCA employed. Unlike many earlier studies, we used quality RCA characterized by lower water absorption and only marginal deviations in LAA and AIV when compared to NCA. This underscores the critical importance of considering the quality of RCA when aiming for better performance in recycled aggregate concrete formulations.

4 Numerical Analysis

A 3D non-linear Finite Element Model is presented to analyze RCA concrete cube and cylinder specimen subjected to compression load (Compression test and split tensile test) to obtain its ultimate compressive

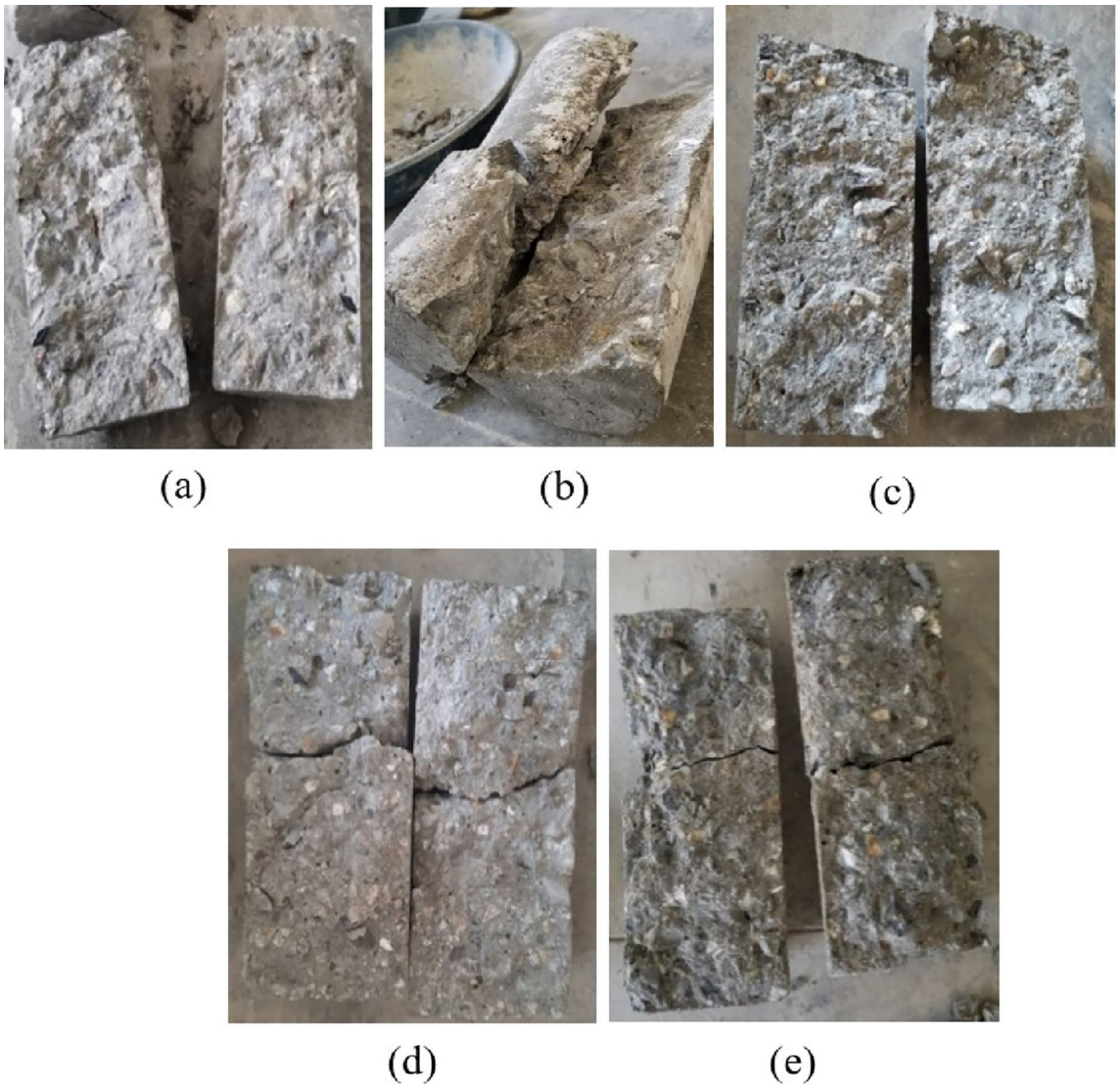

Fig. 12 Fracture patterns for split tensile strength for different concrete mix: **a** R0, **b** R25, **c** R50, **d** R75 and **e** R100

and tensile strength using FEA after obtaining laboratory/ experimental values. To achieve a good result in terms of the material's final load carrying capacity, it is necessary to take into consideration damage criteria and analytical techniques for Nonlinear finite element analysis. (Abaqus 2016 Documentation, 2016) distinguishes itself through three key concrete crack models: the concrete model, brittle crack concrete model, and the potent Concrete Damaged Plasticity (CDP) model. The CDP model is commonly employed for the analysis of concrete damage and fracturing among the diverse models available (Nguyen & Livaoğlu, 2020), (Park et al., 2023).

Significant advancements in concrete modeling have been achieved through extensive research aimed at predicting behavior, crack propagation, and micro crack coalescence. (Lei et al., 2023) have contributed by

Table 7 Split tensile strength test results of concrete

Concrete mix	Average tensile strength (MPa)	
	7 days	28 days
R0	1.46	2.16
R25	1.80	2.56
R50	1.75	2.36
R75	1.55	2.15
R100	1.45	2.13

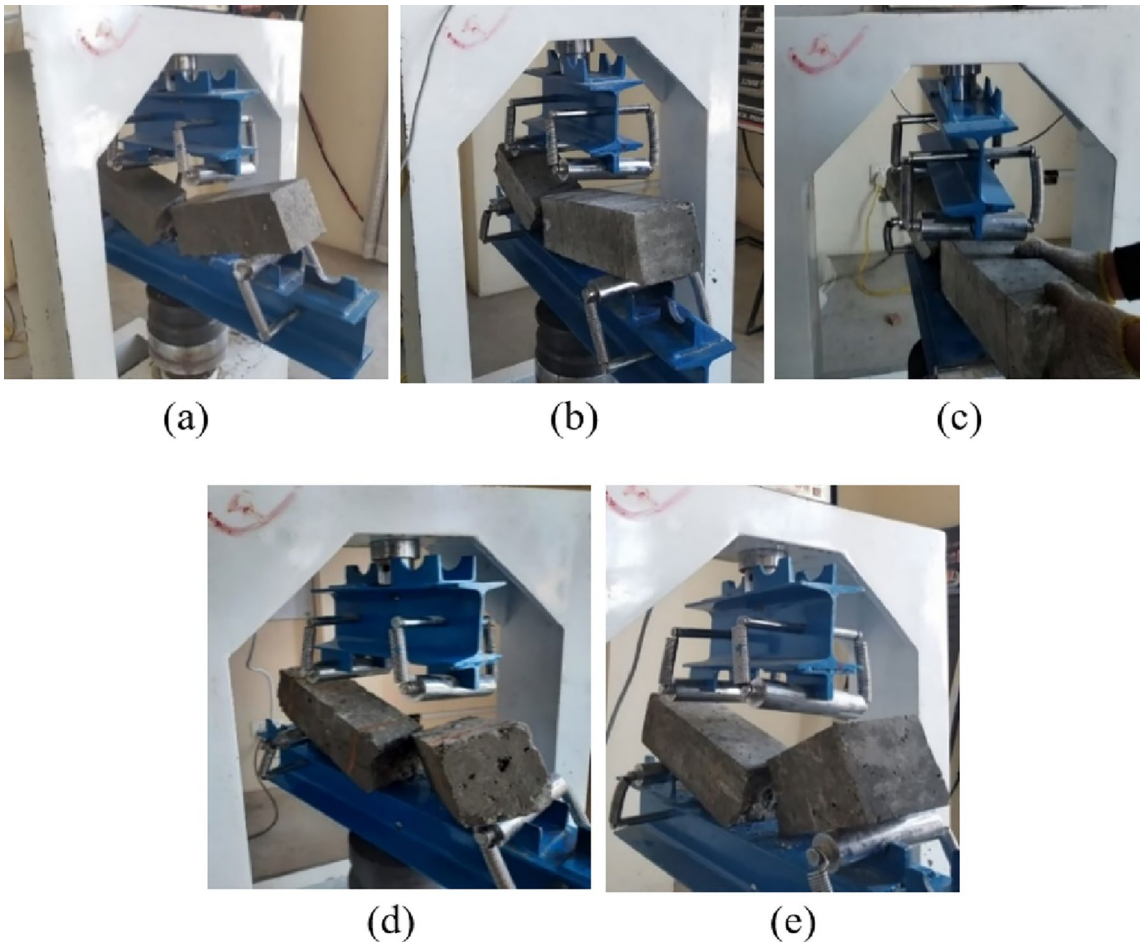

Fig. 13 Four point bending test in laboratory; **a** R0, **b** R25, **c** R50, **d** R75 and **e** R100

introducing an enhanced model within the theoretical framework of the CDP model, specifically tailored for modeling concrete under both monotonic and cyclic triaxial compression. Le Minh et al., (2021) further explored the application of CDP, focusing on simulating the behavior of high-strength concrete under static and dynamic loading conditions within the ABAQUS software. Kaushik et al., (2022) conducted a comprehensive numerical and experimental study to identify optimal values for CDP model parameters, aiming to enhance concrete response against low-velocity impacts. Recognizing the complexity of the CDP theory, Hafezolghorani et al., (2017) simplified the procedure and developed a Simplified Concrete Damaged Plasticity (SCDP) model. Bhatta et al., (2024) also used ABAQUS software to analyze concrete behavior for concrete brick aggregate (CBA). These collective efforts showcase a diverse range of approaches and applications in advancing our understanding of concrete behavior through experimental and numerical investigations.

The present study uses CDP model to simulate the recycled aggregate as it stands out for its adept representation of comprehensive inelastic behavior in both tension and compression, along with seamless compatibility between ABAQUS/STANDARD and ABAQUS/EXPLICIT for efficient result transfer. The CDP model, developed through the research of (Kupfer & Gerstle, 1973) and (Lubliner et al., 1989), serves as a constituent model for concrete materials, enhancing the Drucker-Prager model. Derived from a modified Drucker-Prager strength hypothesis, the CDP model identifies primary concrete failure mechanisms as tensile cracking and comprehensive crushing, offering adaptability across diverse structures and loading conditions (Abaqus 2016 Documentation, 2016). The correlation between the parameters for relative concrete damage in tension and compression is based on stress–strain relationships obtained using experimental methods.

The differences between the result of M20 NAC and RAC were rather small, to calculate CDP as an input

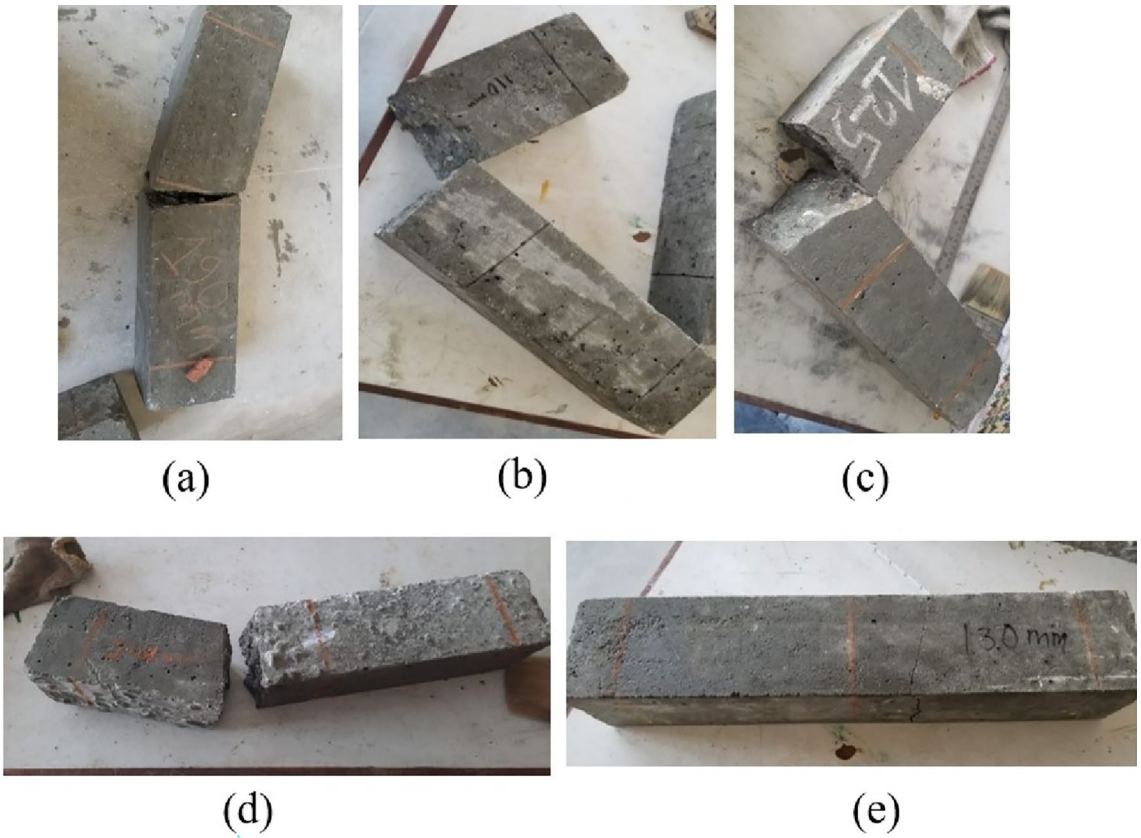

Fig. 14 Fracture patterns for flexure strength test of beam; **a** R0, **b** R25, **c** R50, **d** R75 and **e** R100

Table 8 Modulus of rigidity from flexure strength test of beam

Concrete mix	Distance of crack from near support (a) mm	Average flexure strength (MPa)	
		7 days	28 days
R0	185.83	2.43	3.61
R25	112	2.56	3.79
R50	127	2.45	3.67
R75	142.17	2.42	3.64
R100	130.16	2.27	3.51

variable to the finite element model, material properties required were obtained from Hafezolghorani et al., (2017). In general, for unconfined concrete the uniaxial compressive behavior can be described by either Hognestad (1951.) and Kent and Park (1971). However, this study used the (Kent & Park, 1971) parabolic model, shown in Fig. 18 and the Modified Tension stiffness curve in Fig. 19, for unconfined concrete.

Table 9 Empirical relationship between flexural strength and compressive strength

Equation	Code	Flexure strength from empirical relations (MPa)	Flexure strength from experiment for R0 (MPa)
$f_r = 0.7\sqrt{f_{ck}}$, where, f_{cu} = compressive strength of concrete cubes in MPa	(IS456:, 2000, 2000)	3.77	3.61
$f_r = 7.5\sqrt{f_{ck}\prime}$, where, $f_{ck}\prime$ = compressive strength of concrete cylinder in psi	(ACI318, 2019)	3.11	
$f_r = 0.3f_{ck}^{2/3}$, where, f_{ck} = compressive strength of concrete cylinders in MPa	(Eurocode2, 2004)	2.56	

Table 10 Unit weight of different variation of RCA

Concrete mix	Average unit weight (kN/m^3)	
	7 days	28 days
R0	23.93	24.01
R25	23.82	23.95
R50	23.26	23.35
R75	22.97	23.16
R100	22.73	22.88

For the Uniaxial compressive behavior Kent and Park Parabolic constitutive model, expressed the following equation:

$$\sigma_c = \sigma_{cu}\left[2\left(\frac{\varepsilon_c}{\varepsilon_c'}\right) - \left(\frac{\varepsilon_c}{\varepsilon_c'}\right)^2\right]. \quad (1)$$

where, σ_c = nominal compressive stress, ε_c = nominal compressive strain, σ_{cu} = ultimate compressive stress, ε_c' = ultimate compressive strain of the unconfined cylinder specimen.

Kent and Park, (1971) reported that ε_c' equaled 0.002.

Fig. 18 illustrates a parabolic increase (A, B) during the hardening stage, followed by a linear decrease (B, C) during the softening stage for both confined and unconfined concretes. The stress value at 0.5 σ_{cu}, highlighted in Fig. 18, is significant because it, along with the associated strain ($\varepsilon_{0.5}$, strain in the linear stage), marks the

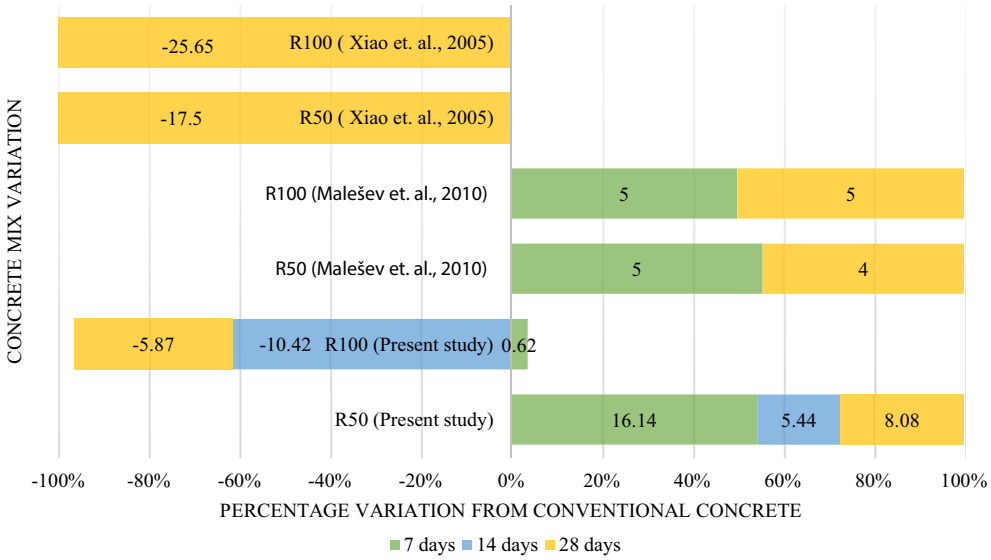

Fig. 15 Percentage variation of compressive strength test of RAC with conventional concrete from present study and previous literature

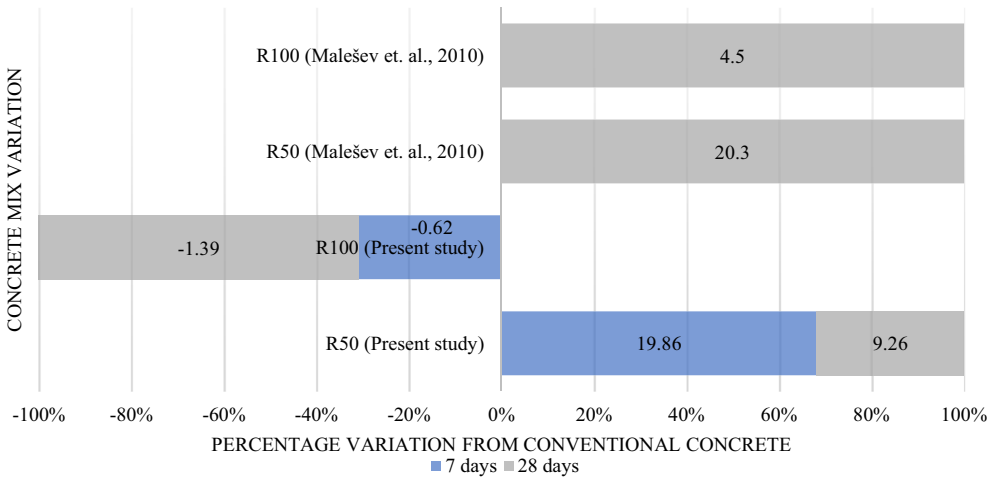

Fig. 16 Percentage variation of split tensile strength of RAC with conventional concrete from present study and previous literature

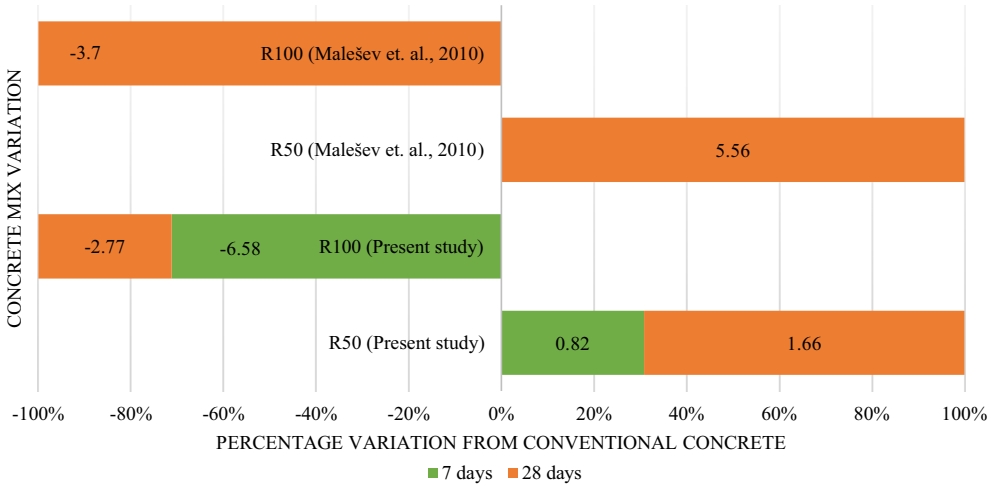

Fig. 17 Percentage variation of flexure strength of RAC with conventional concrete from present study and previous literature

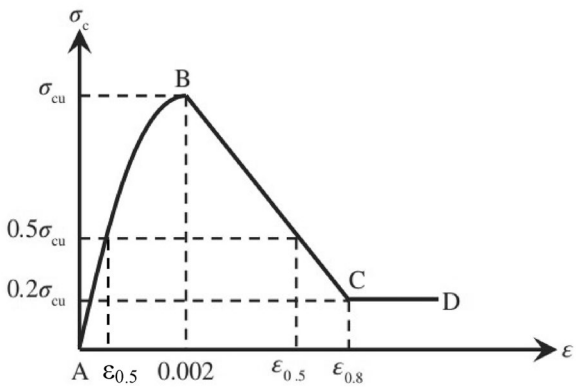

Fig. 18 Kent and Park model for confined and unconfined concrete

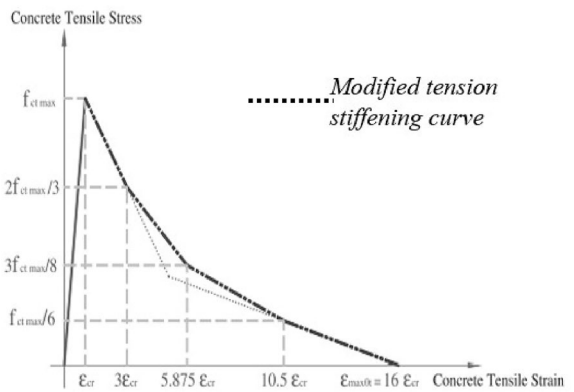

Fig. 19 Modified tension softening curve

transition from the initial linear behavior to the hardening stage in the concrete's stress–strain curve. The softening phase continued until the stress dropped to 20% of the unconfined cylinder compressive strength (Point C). Beyond this point, the stress was prevented from further decreasing, and perfect plastic behavior was assumed along the softening path (C, D). For simplicity, the entire constitutive model was approximated as a parabolic curve. Equation (1) captures the nonlinear behavior of concrete from start to finish (Hafezolghorani et al., 2017).

The inelastic hardening strain in compression was derived as,

$$\varepsilon_c^{in,h} = \varepsilon_c - \frac{\sigma_c}{E_c}. \quad (2)$$

Concrete under tension was modeled as a linear elastic brittle material with strain softening.

As suggested by (Allam et al., 2013), a modified tension softening curve (Fig. 19) was used to permit a relatively gradual response behavior and consequently to decrease the convergence problem. The Compressive strength (f_{ck}) and tensile strength (f_{ct}) of concrete cylinders obtained from 28 days tests as shown in Tables 6 and 7, were used to calculate the CDP parameters, denoted by σ_{cu} and f_{ct}. Poisson's ratio for concrete typically ranges from 0.1 to 0.2; in the study, a value of 0.2 was used.

The modulus of elasticity (E) has been calculated from the formula

$$(E) = 5000\sqrt{f_{ck}}\,\text{MPa} \quad (3)$$

where, f_{ck} is the compressive strength of cylinder tested at 28 days of curing from Table 6.

The constitutive plastic parameters used for the ABAQUS2017 simulation of a concrete has been taken as per (Hafezolghorani et al., 2017).

The dilation angle reflects a material's ability to deform under stress, with a higher dilation angle indicating

greater ductility and flexibility. This affects the transition from elastic to plastic behavior in the stress–strain curve. For concrete, the typical dilation angle ranges from 20° to 40°. Adjusting the dilation angle within this range allows for calibration. In this study, a dilation angle of 31° was used.

Flow potential eccentricity influences the curvature of the flow potential, playing a critical role in accurately modeling the material's behavior during the hardening stage. Adjusting this parameter can affect both the onset and the progression of hardening in the stress–strain curve. In this study, the default value of flow potential eccentricity is set at 0.1.

The ratio f_{b0}/f_{c0} which is the ratio of initial equiaxial compressive yield stress to initial uniaxial compressive yield stress, has been set to its default value.

The coefficient K represents the ratio of hydrostatic effective stress on the tensile meridian to that on the compressive meridian when the maximum principal stress is negative. This coefficient influences the plastic deformation behavior of the material under loading conditions. In this study, the suggested value of $K = 0.667$ has been used.

A null value for the viscosity parameter is used by the ABAQUS software to prevent viscoplastic regularization. This approach improves the convergence rate of the model during the softening process and yields good results.

4.1 FEA of Compressive Strength Test of Concrete Cube

The continuum 3-dimensional, eight-noded C3D8R components, which have reduced integration points, were chosen for the ABAQUS model. Constant displacement was used for boundary conditions at the rigid body on top up until failure and encastering of the bottom surface. Concrete crushing issues and spalling have not been taken into account; coupling is described as the interaction of a number of nodes to remove localized stress conditions. In order to minimize the impact and inertia effect of explicit dynamic methods, as well as ensure equal static responses, the loading period was adjusted until minimal Kinetic effects were achieved. The loading period was eventually fixed at 1 s with the initial trial value determined on the basis of the natural frequency of the M20 concrete cube after a process of trial and error.

The ideal mesh density that provides appropriate precision in findings and appropriate time to analyze was found through analysis of models with various mesh refinements. The mesh size of 8 mm and mass density of 2197 elements produced similar results in a reasonable period of time when comparing the compression strengths to the results of the experiment. The results of the FEM are displayed in the Table 11, along with a comparison to the experiment.

The agreement between ABAQUS numerical predictions and laboratory test data for the compressive strength test of the concrete cubes is consistently commendable across all five mixes, with variations consistently below 10%, as detailed in Table 11. Notably, the R75 mix exhibits the highest variation at 5.56%, while the remaining four mixes demonstrate minimal discrepancies. By defining material properties such as compressive and tensile strengths and calibrating key parameters like the dilation angle, flow potential eccentricity, f_{b0}/f_{c0} ratio, and coefficient K based on Hafezolghorani et al., (2017), the model accurately depicted the inelastic behavior of concrete under load. Additionally, using a simplified CDP model and incorporating specific stress–strain relationships from experimental findings ensured that the finite element model (FEM) responses closely mirrored real-world performance (Hafezolghorani et al., 2017). This precise calibration minimized discrepancies between the FEM and experimental results, demonstrating the model's reliability and accuracy in simulating the behavior of RCA concrete.

In both experimental and numerical analysis, similar fracture pattern has been noticed. In Fig. 20, cracks consistently manifest near the edges and along the height of the concrete cubes, propagating towards the center. This uniform crack pattern, characterized by a conical or cone failure, is observed across all five design mixes in both the experimental and numerical studies, which is also evident in Fig. 21. The compression force applied to the

Table 11 Results of compressive strength tests from FEM

Concrete mix	ABAQUS mesh type-size	Total nodes	Total elements	Maximum stress at failure (MPa)		Variation from experiment (%)
				FEM	Experimental	
R0	C3D8R	2744	2197	29.50	28.96	1.86
R25	C3D8R	2744	2197	35.47	34.79	1.95
R50	C3D8R	2744	2197	32.01	31.30	2.3
R75	C3D8R	2744	2197	30.96	29.33	5.56
R100	C3D8R	2744	2197	27.65	27.26	1.43

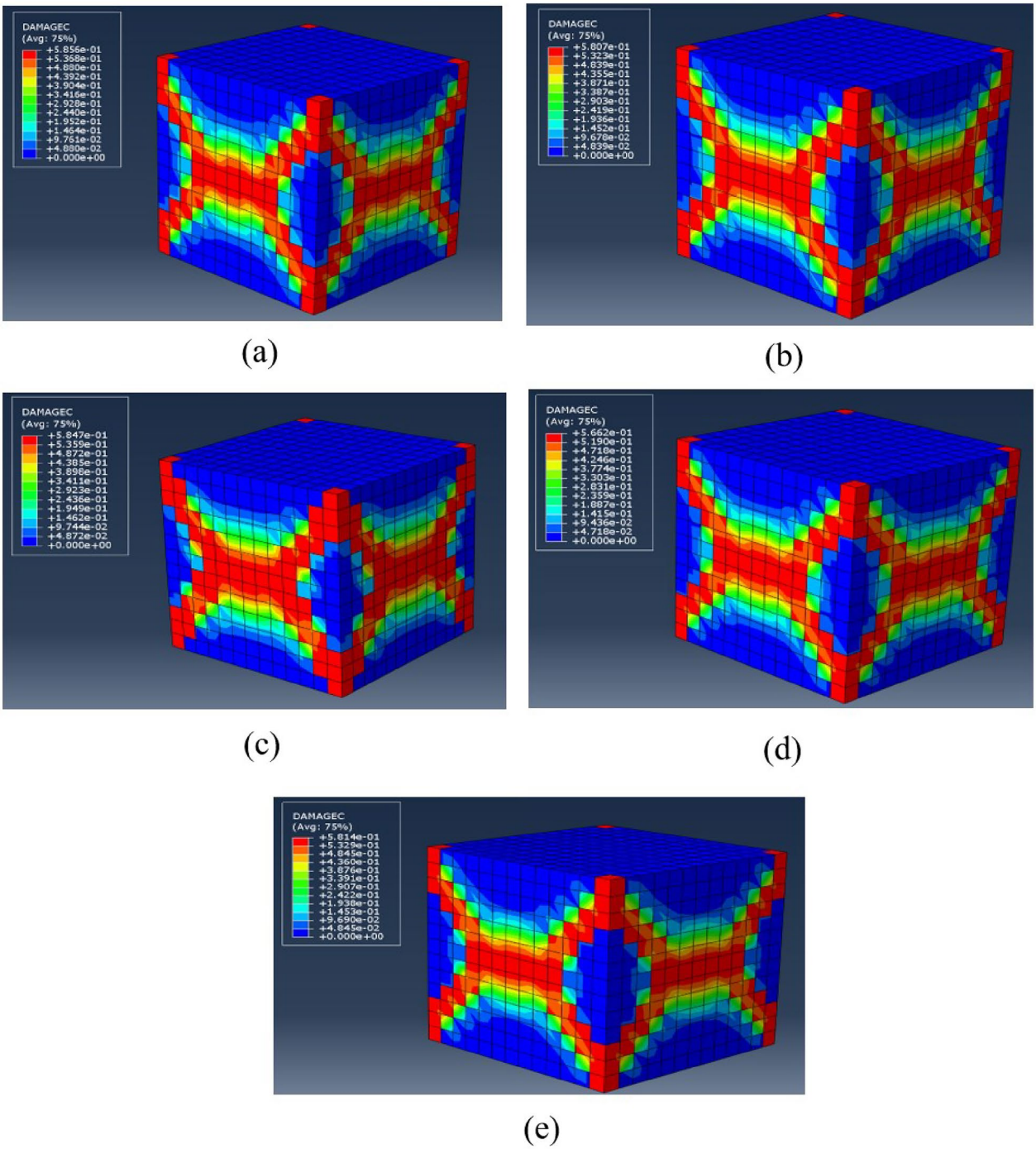

Fig. 20 Crack patterns of cube obtained from FEA different concrete mix; **a** R0, **b** R25, **c** R50, **d** R75 and **e** R100

concrete cube causes it to expand at the middle height, contributing to this consistent failure pattern.

4.2 FEA of Split Tensile Strength of Concrete Cylinders

A C3D8R element, Continuum 3-Dimensional, eight noded and reduced integration point were selected in ABAQUS model. For the analysis, a uniform mesh size of 8 mm (Global Mesh size) has been chosen. In accordance with the boundary conditions, constant displacement was applied on top of the rigid body until a failure occurs and the bottom surface is anchored. The split was

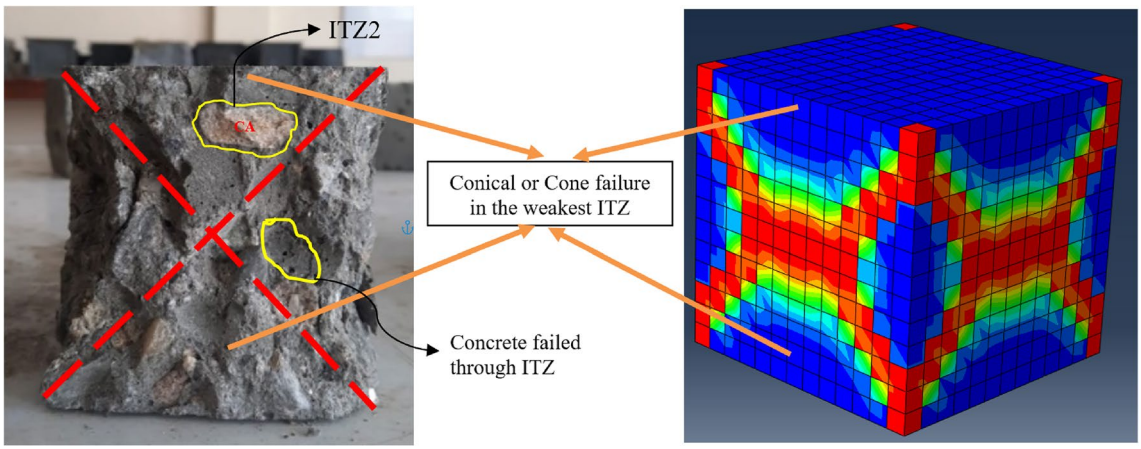

Fig. 21 Experimental and numerical analysis comparison for crack of compressive strength test of cube

provided with constraint condition: tie and meshed with size 5 (Global Mesh size).

The analysis of models with various mesh refinements has identified optimal mesh density, which shall allow accurate findings and reasonable analyses time. When Split Tensile strength was compared to the results of the experiment, the mesh size of 8 mm and the mesh density of 13072 elements produced the same results as the experiment in a fair amount of time. The results of the FEM are displayed in the Table 12, along with a comparison to the experiment.

The split tensile test of concrete cylinders reveals a commendable level of agreement, with variations below 10% between ABAQUS numerical predictions and laboratory test data for all five concrete mixes. Notably, R25 exhibits the highest variation at 7.5% among the mixes.

The close agreement between experimental and numerical results was achieved by using the CDP model in ABAQUS, which effectively captures the nonlinear behavior of concrete under various loading conditions. The model parameters were derived from experimental data and validated against established constitutive models like those of Kent and Park. Additionally, the mesh density was optimized to balance computational efficiency and accuracy. Consistency in the boundary conditions and precise control of loading rates also helped minimize discrepancies. Although concrete's heterogeneous nature typically introduces variability, the rigorous approach to FEM calibration and the controlled experimental setup led to consistent results.

Fig. 22 illustrates consistent fracture patterns for all mixes in the ABAQUS simulations, with each cylinder displaying the same splitting pattern. A detailed comparison of crack patterns in Fig. 23 showcases the congruence between laboratory observations and ABAQUS simulations, emphasizing the consistent splitting of cylinders into two parts.

In the course of the split tensile test, the initiation of cracks at the center of the specimen due to induced tensile stresses from diametrical loading results in outward propagation. This stress distribution ultimately gives rise to a perpendicular plane of failure, leading to the characteristic splitting of concrete cylinders into two halves. In the study, transverse cracks has been seen formed after longitudinal cracks due to stress redistribution. Initially, the applied load induces tensile stress along the vertical plane, causing a longitudinal crack. This crack relieves some stress, but the remaining uncracked sections still bear the load, creating secondary transverse tensile stresses. As concrete is brittle with low tensile strength, these redistributed stresses can exceed its capacity, leading to additional transverse cracks. Thus, the initial longitudinal crack indicates primary tensile failure, while transverse cracks reflect the material's response to continued loading and stress redistribution. The noted agreement between numerical predictions and experimental outcomes not only underscores the precision of ABAQUS in emulating real-world behavior but also positions this test as an invaluable tool for gaining profound insights into the tensile strength of concrete.

The stress–strain curve obtained from compressive strength test of cube in ABAQUS is shows in Fig. 24.

The tensile strength vs. displacement plot from ABAQUS is shown in Fig. 25.

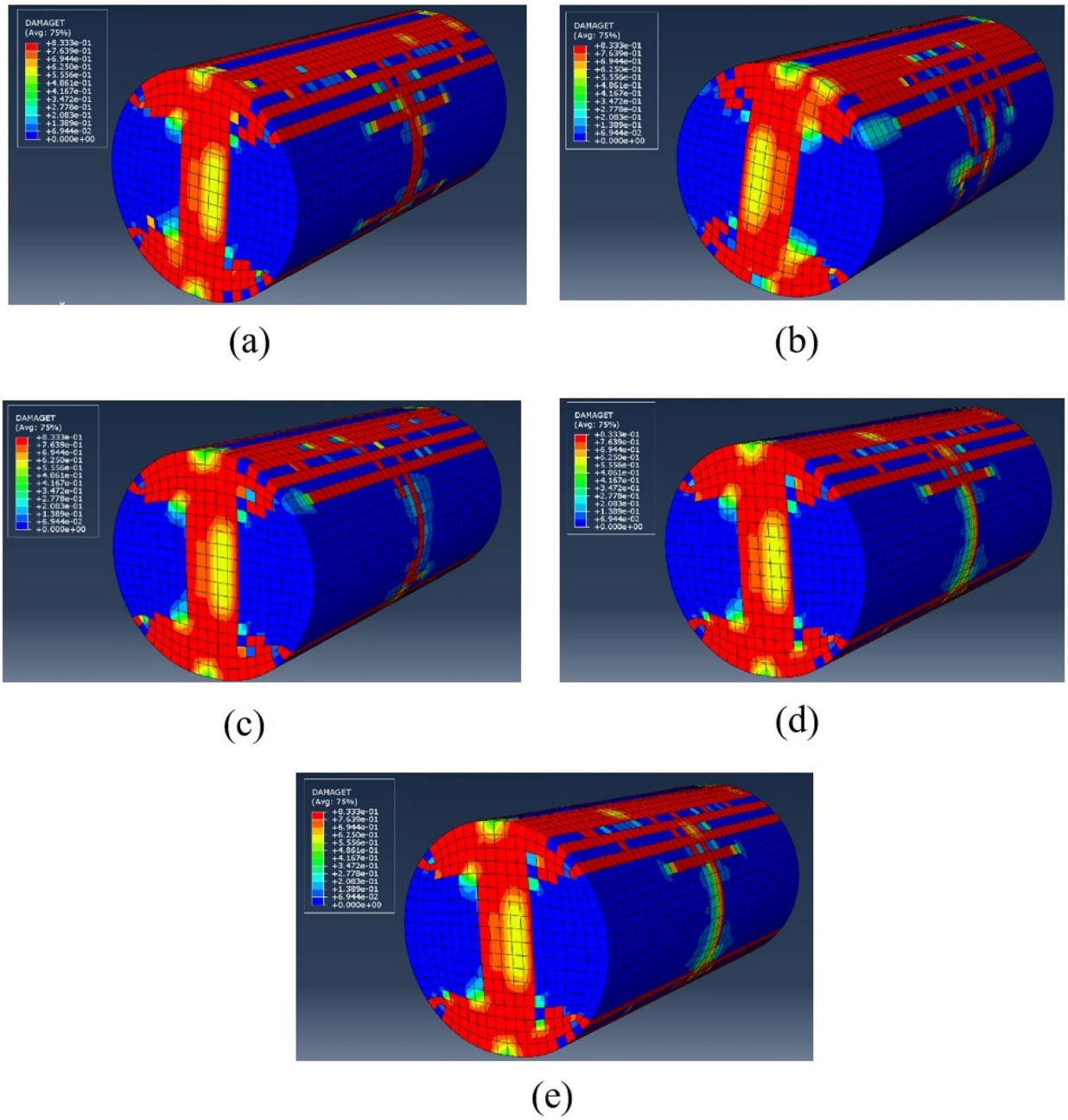

Fig. 22 Crack patterns of cylinder obtained from FEA for different concrete mix; **a** R0, **b** R25, **c** R50, **d** R75 and **e** R100

5 Conclusion

The increasing global production of concrete poses considerable environmental challenges, particularly concerning water consumption, depletion of natural aggregates, and the overall increase in concrete output. Addressing the pressing issue of accumulated demolished waste, this research strongly advocates for sustainable practices, with a specific focus on the utilization of RCA. The study centers around the reusability of Demolished Concrete, examining mechanical properties, crack patterns, strength variations, and specific gravity evaluations for different RCA compositions. This comprehensive investigation underscores the ongoing efforts toward sustainable concrete practices and presents critical findings based on a comparative analysis of test results involving five different percentages of coarse recycled aggregate content (0%, 25%, 50%, 75%, and 100%).

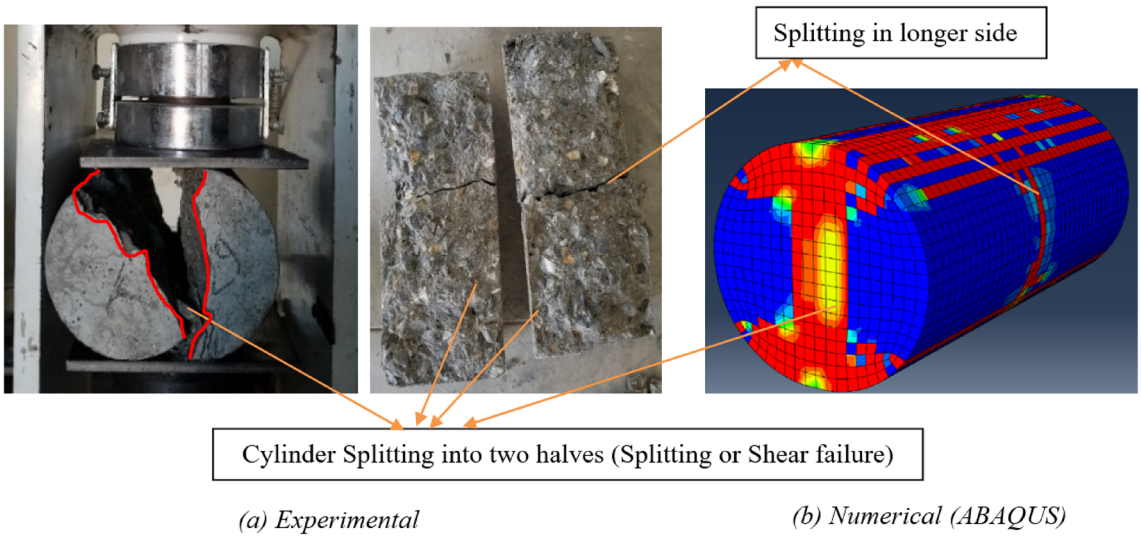

Fig. 23 Experimental and numerical analysis comparison for crack of split tensile strength test of cylinder

Table 12 Results of split tensile strength test

Concrete mix	ABAQUS mesh type-size	Total nodes	Total elements	Maximum stress at failure (MPa)		Variation from experiment (%)
				FEM	Experimental	
R0	C3D8R	14625	13072	2.075	2.16	3.9
R25	C3D8R	14625	13072	2.367	2.56	7.5
R50	C3D8R	14625	13072	2.229	2.36	5.55
R75	C3D8R	14625	13072	2.068	2.15	3.81
R100	C3D8R	14625	13072	2.026	2.13	4.88

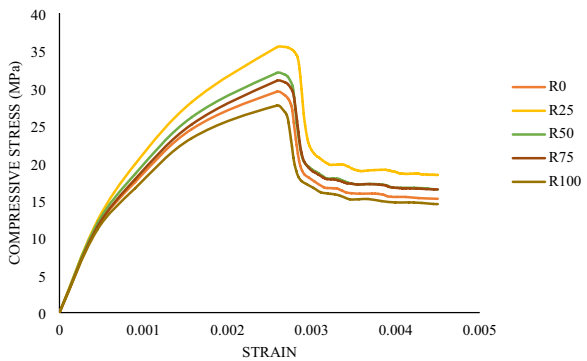

Fig. 24 Stress–strain curve from compressive strength of cube in ABAQUS

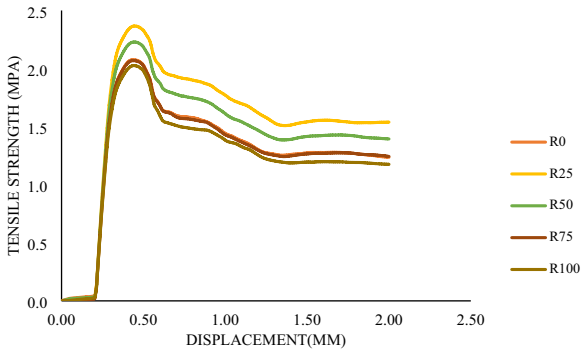

Fig. 25 Tensile strength vs. displacement plot from ABAQUS

1. In terms of compressive strength of cube, the study reveals significant improvements for R25, R50, and R75, with increases of 20.13%, 8.08%, and 1.28%, respectively. However, R100 experiences a decrease of 5.87% compared to R0 in tests performed at 28 days of curing.
2. The compressive strength of cylinder showed an increase of 25.86%, 18.88%, 9.54% and 2.65% for R25, R50, R75 and R100 concrete mix as compared to R0 mix for the test performed at 28 days of curing.

3. The current study found out the ratio of compressive strength for cylinder to cube in the range of 0.9–0.95.
4. Tensile strength at the same curing period shows positive outcomes for R25 and R50, exhibiting increases of 18.52% and 9.26%, while R75 and R100 witness decreases of 0.46% and 1.39%, respectively.
5. Flexural strength displays a similar trend, with increases for R25, R50, and R75 by 5%, 1.66%, and 0.83%, respectively, and a decrease of 2.77% for R100 compared to R0.
6. The introduction of RCA positively influences compressive, tensile, and flexural strength, with the highest performance observed in R25, featuring 25% RCA and 75% Natural Aggregate. This is attributed to the quality of RCA used in the study.
7. In the flexure strength test, R25 demonstrates a shorter distance between the nearest support and the fracture plane, indicating weaker bonding farther from the beam's middle point than other variations.
8. A examination of physical and mechanical characteristics reveals disparities between natural coarse aggregate and recycled aggregates, including a decrease in specific gravity and an increase in water absorption, Los Angeles Abrasion Value, and Aggregate Impact Values.
9. Furthermore, increasing recycled aggregate content (RAC) correlates with a slight reduction in concrete bulk density.
10. Numerical analysis, employing the Kent and Park Model, consistently produces similar fracture patterns across all five concrete mixtures during compressive and split tensile strength tests.
11. The difference in compressive strength from numerical and experimental analysis for R0, R25, R50, R75 and R100 found to be 1.86%, 1.95%, 2.3%, 5.56% and 1.43%, respectively, while for split tensile test the discrepancies has been found to be 3.9%, 7.5%, 5.5%, 3.81% and 4.88%, respectively.
12. These variations signify the accuracy and reliability of the numerical simulations in replicating the real-world performance of the different concrete compositions.

In conclusion, this study's comprehensive findings on the properties of fresh and hardened concrete strongly recommend using recycled aggregate concrete. Specifically, R25 is identified as an optimal alternative for achieving the maximum strength of an M20 concrete design mix, while R75 is suggested for applications aiming to maximize the use of demolished concrete, showing promising results. The numerical analysis using the Kent and Park Model consistently reveals similar fracture patterns across all five concrete mixtures during both compressive and split tensile strength tests. The fracture plane consistently identifies the weakest Interfacial Transition Zone (ITZ) due to deficient bond strength and increased porosity. As the load is applied, stress concentration occurs in both ITZ1 and ITZ2, ultimately leading to failure. However, while these observations suggest the role of ITZs in failure mechanisms, our conclusions are based on trends rather than definitive evidence. Further detailed studies, including advanced simulations and experimental observations, are required to conclusively demonstrate the failure surface propagation along ITZs.

This research significantly contributes valuable insights into sustainable construction practices, emphasizing the potential of RCA to mitigate the environmental impact associated with traditional concrete production. The present study has certain limitations that future research should address. It is highly recommended to evaluate the long-term durability performance of concrete containing demolished concrete and to conduct structural studies assessing the behavior and performance of reinforced concrete elements or structural members made with demolished concrete. These areas of focus will provide a more comprehensive understanding of the potential and limitations of using recycled concrete aggregates in sustainable construction practices.

Acknowledgements
The authors gratefully acknowledge Department of Civil Engineering, Kathmandu University for providing research opportunity and access to their laboratory facilities.

Author contributions
BN: conceptualization, methodology, idea of research, conduct experiment, analysis of the test results, drafted manuscript. KS: conceptualization, idea of research writing, review, supervision and editing. SSK: conceptualization, idea of research writing, review, supervision and editing.

Funding
This research received no external funding.

Availability of data and materials
All data generated and analysis during this study are included in this article.

Declarations

Competing interests
The authors declare that there is no conflict of intertest regarding this publication.

Received: 25 December 2023 Accepted: 29 September 2024
Published online: 13 January 2025

References

Abaqus 2016 Documentation. (2016). http://130.149.89.49:2080/v2016/index.html

ACI 318. (2019). Buiisding code requirements for structural concrete (ACI 318–19) and commentary (ACI 318R-19).
Allam, S. M., Shoukry, M. S., Rashad, G. E., & Hassan, A. S. (2013). Evaluation of tension stiffening effect on the crack width calculation of flexural RC members. *Alexandria Engineering Journal, 52*(2), 163–173. https://doi.org/10.1016/J.AEJ.2012.12.005
Bhatta, N., Adhikari, A., Ghimire, A., Bhandari, N., Subedi, A., & Sahani, K. (2024). Comparing crushed brick as coarse aggregate substitute in concrete: experimental vs. numerical study. *Iranian Journal of Science and Technology Transactions of Civil Engineering*. https://doi.org/10.1007/S40996-024-01407-8/METRICS
Bravo, M., De Brito, J., Pontes, J., & Evangelista, L. (2015). Durability performance of concrete with recycled aggregates from construction and demolition waste plants. *Construction and Building Materials, 77*, 357–369. https://doi.org/10.1016/J.CONBUILDMAT.2014.12.103
De Brito, J., Agrela, F., & Silva, R. V. (2019). Construction and demolition waste. In J. De Brito, F. Agrela, & R. V. Silva (Eds.), *New trends in eco-efficient and recycled concrete* (pp. 1–22). Amsterdam: Elsevier.
Buck, A. D. (1977). Recycled concrete as a sourceof aggregate. *Journal of the Ameriacan Concrete Institute, 74*(5), 212–219. https://doi.org/10.14359/11004
Corinaldesi, V. (2011). Structural concrete prepared with coarse recycled concrete aggregate: From investigation to design. *Advances in Civil Engineering*. https://doi.org/10.1155/2011/283984
de Juan, M. S., & Gutiérrez, P. A. (2009). Study on the influence of attached mortar content on the properties of recycled concrete aggregate. *Construction and Building Materials, 23*(2), 872–877. https://doi.org/10.1016/J.CONBUILDMAT.2008.04.012
Etxeberria, M., Vázquez, E., Marí, A., & Barra, M. (2007). Influence of amount of recycled coarse aggregates and production process on properties of recycled aggregate concrete. *Cement and Concrete Research, 37*(5), 735–742. https://doi.org/10.1016/J.CEMCONRES.2007.02.002
Eurocode 2. (2004). Design of concrete structures—part 1-1: General rules and rules for buildings (EN 1992-1-1:2004). European Committee for Standardization.
Evangelista, L., & de Brito, J. (2010). Durability performance of concrete made with fine recycled concrete aggregates. *Cement and Concrete Composites, 32*(1), 9–14. https://doi.org/10.1016/J.CEMCONCOMP.2009.09.005
Gagg, C. R. (2014). Cement and concrete as an engineering material: An historic appraisal and case study analysis. *Engineering Failure Analysis, 40*, 114–140. https://doi.org/10.1016/J.ENGFAILANAL.2014.02.004
Gonzalez-Valencia, R., Magana-Rodriguez, F., Cristóbal, J., & Thalasso, F. (2016). Hotspot detection and spatial distribution of methane emissions from landfills by a surface probe method. *Waste Management, 55*, 299–305. https://doi.org/10.1016/J.WASMAN.2016.03.004
Gyawali, T. R. (2022). Re-use of concrete/brick debris emerged from big earthquake in recycled concrete with zero residues. *Cleaner Waste Systems, 2*, 100007. https://doi.org/10.1016/J.CLWAS.2022.100007
Hafezolghorani, M., Hejazi, F., Vaghei, R., Jaafar, M. S. B., & Karimzade, K. (2017). Simplified damage plasticity model for concrete. *Structural Engineering International, 27*(1), 68–78. https://doi.org/10.2749/101686616X1081
Hognestad, Eivind. (1951). A study of combined bending and axial load in reinforced concrete members. Reinforced concrete research council of the engineering foundation
IS 383. (2016). Specification for coarse and fine aggregates from natural sources for concrete. Bureau of Indian Standard. New Delhi, Reaffirmed 2005
IS 456:2000. (2000). Plain and reinforced concrete—code of practice (IS 456:2000). Bureau of Indian Standards
IS 516. (1959). Methods of tests for strength of concrete. Bureau of Indian Standard, Reaffirmed 2004
IS 5816. (1999). Splitting tensile strength of concrete: Method of test. Bureau of Indian Standard, Reaffirmed 2004
IS 2386-Part I. (1963). Methods of test for aggregates for concrete: Particle size and shape. Bureau of Indian Standard, Reaffirmed 2002
IS 2386-Part III. (1963). Methods of test for aggregates for concrete: specific gravity, density, voids, absorption and bulking. Bureau of Indian Standard, Reaffirmed 2002
IS 2386-Part IV. (1963). Methods of test for aggregates for concrete: Mechanical properties. Bureau of Indian Standard, Reaffirmed 2022
IS 4031- Part 1. (1996). Method of physical tests for hydraulic cement: Determination of fineness by dry sieving. Bureau of Indian Standards, New Delhi, Reaffirmed in 2005
IS 4031-Part 3. (1988). Methods of physical tests for hydraulic cement : Determination of soundness. Bureau of Indian Standards, New Delhi, Reaffirmed in 2005
IS 4031-Part 4. (1988). Methods of physical tests for hydraulic cement :Determination of consistency of standard cement paste. Bureau of Indian Standards, New Delhi, Reaffirmed 2005
IS 4031-Part 5. (1988). Methods of physical tests for hydraulic cement : Determination of initial and final setting times. Bureau of Indian Standards, New Delhi, Reaffirmed in 2005
IS 10262. (2019). Concrete mix proportioning—guidelines, Bureau of Indian Standard, second revision
Kalinowska-Wichrowska, K., Pawluczuk, E., Bołtryk, M., Jimenez, J. R., Fernandez-Rodriguez, J. M., & Morales, D. S. (2022). The performance of concrete made with secondary products—recycled coarse aggregates, recycled cement mortar, and fly ash-slag mix. *Materials*. https://doi.org/10.3390/ma15041438
Kaushik, A., Patnaik, G., Rajput, A., & Prakash, G. (2022). Nonlinear behaviour of concrete under low-velocity impact by using a damaged plasticity model. *Iranian Journal of Science and Technology Transactions of Civil Engineering, 46*(5), 3655–3677. https://doi.org/10.1007/S40996-021-00808-3/METRICS
Kent, D., & Park, R. (1971). Flexural members with confined concrete. *Journal of the Structural Division*. https://doi.org/10.1061/JSDEAG.0002957
Kupfer, H. B., & Gerstle, K. H. (1973). Behavior of concrete under biaxial stresses. *Journal of the Engineering Mechanics Division, 99*(4), 853–866. https://doi.org/10.1061/JMCEA3.0001789
Le Minh, H., Khatir, S., Abdel Wahab, M., & Cuong-Le, T. (2021). A concrete damage plasticity model for predicting the effects of compressive high-strength concrete under static and dynamic loads. *Journal of Building Engineering, 44*, 103239. https://doi.org/10.1016/J.JOBE.2021.103239
Lei, B., Qi, T., Li, Y., Jin, Z., & Qian, W. (2023). An enhanced damaged plasticity model for concrete under cyclic and monotonic triaxial compression. *European Journal of Mechanics A/Solids, 100*, 104999. https://doi.org/10.1016/J.EUROMECHSOL.2023.104999
Li, W., Xiao, J., Sun, Z., Kawashima, S., & Shah, S. P. (2012). Interfacial transition zones in recycled aggregate concrete with different mixing approaches. *Construction and Building Materials, 35*, 1045–1055. https://doi.org/10.1016/j.conbuildmat.2012.06.022
Lubliner, J., Oliver, J., Oller, S., & Oñate, E. (1989). A plastic-damage model for concrete. *International Journal of Solids and Structures, 25*(3), 299–326. https://doi.org/10.1016/0020-7683(89)90050-4
Makul, N. (2021). A review on methods to improve the quality of recycled concrete aggregates. *Journal of Sustainable Cement-Based Materials*. https://doi.org/10.1080/21650373.2020.1748742
Malešev, M., Radonjanin, V., & Marinković, S. (2010). Recycled concrete as aggregate for structural concrete production. *Sustainability, 2*(5), 1204–1225. https://doi.org/10.3390/SU2051204
Memon, S. A., Bekzhanova, Z., & Murzakarimova, A. (2022). A review of improvement of interfacial transition zone and adherent mortar in recycled concrete aggregate. *Buildings*. https://doi.org/10.3390/buildings12101600
NBC 105:2020. (2020). Seismic design of buildings on Nepal, Nepal Building Code, Kathmandu, Nepal.
Nguyen, Q. T., & Livaoğlu, R. (2020). The effect of the ratio of Λ-shaped shear connectors on the flexural behavior of a reinforced concrete frame. *Advances in Structural Engineering, 23*(12), 2724–2740. https://doi.org/10.1177/1369433220920442
Oikonomou, N. D. (2005). Recycled concrete aggregates. *Cement and Concrete Composites, 27*(2), 315–318. https://doi.org/10.1016/j.cemconcomp.2004.02.020
Otsuki, N., Miyazato, S., & Yodsudjai, W. (2003). Influence of recycled aggregate on interfacial transition zone, strength, chloride penetration and carbonation of concrete. *Journal of Materials in Civil Engineering, 15*(5), 443–451. https://doi.org/10.1061/(asce)0899-1561(2003)15:5(443)
Park, H. W., Lee, J. H., & Jeong, J. H. (2023). Finite element analysis of continuously reinforced bonded concrete overlay pavements using the concrete damaged plasticity model. *Sustainability, 15*(6), 4809. https://doi.org/10.3390/su15064809

Post disaster needs assessment. (2015). www.npc.gov.np
Rahal, K. (2007). Mechanical properties of concrete with recycled coarse aggregate. *Building and Environment, 42*(1), 407–415. https://doi.org/10.1016/J.BUILDENV.2005.07.033
Sagoe-Crentsil, K. K., Brown, T., & Taylor, A. H. (2001). Performance of concrete made with commercially produced coarse recycled concrete aggregate. *Cement and Concrete Research, 31*(5), 707–712. https://doi.org/10.1016/S0008-8846(00)00476-2
Silva, R. V., De Brito, J., & Dhir, R. K. (2014). Properties and composition of recycled aggregates from construction and demolition waste suitable for concrete production. *Construction and Building Materials, 65*, 201–217. https://doi.org/10.1016/j.conbuildmat.2014.04.117
Srivastava V., Singh S. K., & Kumar A. (2015). Stone dust and recycled aggregate in concrete—effect on compressive strength. www.ijert.org
Tabsh, S. W., & Abdelfatah, A. S. (2009). Influence of recycled concrete aggregates on strength properties of concrete. *Construction and Building Materials, 23*(2), 1163–1167. https://doi.org/10.1016/J.CONBUILDMAT.2008.06.007
Tam, V. W. Y., Soomro, M., & Evangelista, A. C. J. (2018). A review of recycled aggregate in concrete applications (2000–2017). *Construction and Building Materials, 172*, 272–292. https://doi.org/10.1016/j.conbuildmat.2018.03.240
Volz J. S., Khayat K. H., Arezoumandi M., & Sadati S. (2014). Recycled concrete aggregate (RCA) for infrastructure elements. https://www.researchgate.net/publication/281232843
Xiao, J., Li, J., & Zhang, C. (2005). Mechanical properties of recycled aggregate concrete under uniaxial loading. *Cement and Concrete Research, 35*(6), 1187–1194. https://doi.org/10.1016/J.CEMCONRES.2004.09.020
Yehia, S., Abdelfatah, A., & Mansour, D. (2020). Effect of aggregate type and specimen configuration on concrete compressive strength. *Crystals, 10*(7), 625. https://doi.org/10.3390/CRYST10070625
Yue, G., Ma, Z., Liu, M., Liang, C., & Ba, G. (2020). Damage behavior of the multiple ITZs in recycled aggregate concrete subjected to aggressive ion environment. *Construction and Building Materials*. https://doi.org/10.1016/j.conbuildmat.2020.118419
Zaharieva, R., Buyle-Bodin, F., Skoczylas, F., & Wirquin, E. (2003). Assessment of the surface permeation properties of recycled aggregate concrete. *Cement and Concrete Composites, 25*(2), 223–232. https://doi.org/10.1016/S0958-9465(02)00010-0
Zhang, H., Ji, T., & Liu, H. (2019). Performance evolution of the interfacial transition zone (ITZ) in recycled aggregate concrete under external sulfate attacks and dry-wet cycling. *Construction and Building Materials*. https://doi.org/10.1016/j.conbuildmat.2019.116938
Zhang, Y., Chen, X., Zhou, J., Huang, J., & Wang, Q. (2021). Interfacial transition zone characteristics of recycled concrete: A review. *IOP Conference Series: Earth and Environmental Science*. https://doi.org/10.1088/1755-1315/692/4/042051

Publisher's Note

Bini Neupane Student at the Department of Civil Engineering, Kathmandu University, Dhulikhel, Nepal

Kameshwar Sahani Assistant Professor at the Department of Civil Engineering, Kathmandu University, Dhulikhel, Nepal

Shyam Sundar Khadka Associate Professor at the Department of Civil Engineering, Kathmandu University, Dhulikhel, Nepal